STUDIES OF INORGANIC NANOPARTICLES AS COLLECTORS FOR FLOTATION

STUDIES OF INORGANIC NANOPARTICLES AS COLLECTORS FOR FLOTATION

By

BEHNAM NADERIZAND, B.ENG

A Thesis

Submitted to the School of Graduate Studies

In Partial Fulfillment of the Requirements

For the Degree

Master of Applied Science

McMaster University

Master of Applied Science (2010) McMaster University

Chemical Engineering Hamilton, Ontario

TITLE: Studies of inorganic nanoparticles as collectors for flotation

AUTHOR: Behnam Naderizand
B.Eng. (Amirkabir University of Technology, Iran)

SUPERVISOR: Professor Robert H. Pelton

NUMBER OF PAGERS: 69

Abstract

The goal of my work was to synthesize an appropriate inorganic nanoparticle as a collector for flotation of glass beads and also to prepare thin films of nickel sulfide. The first step was preparing a very uniform thin layer of nickel sulfide for model adhesion studies. The method employed was successive ionic layer adsorption and reaction (SILAR). The characterization experiments showed a weak deposited layer of nickel sulfide on glass, which was very uneven at low SILAR deposition cycles and very porous at high SILAR deposition cycles.

In the next step, commercial grades of precipitated calcium carbonate (PCC) and colloidal silica were employed as collectors for the flotation of glass beads. Also, stearic acid treatments were carried out on untreated PCC samples. Despite that the mean particle size of PCC particles were in the nano range, they aggregated in aqueous solution and particle size increased to the micron range. Therefore, deposition of these particles onto glass beads was very low and consequently flotation results were not satisfactory. Also, silica particles aggregated when the pH increased to 9 which is the flotation operating pH. These particles did not show good deposition onto glass beads nor good flotation ability. The reasons could be hydrophilicity and aggregation of colloidal silica.

In another series of experiments, stearic acid treated PCC nanoparticles were synthesized with a carbonation method and characterized with electrophoretic mobility, dynamic light scattering, FTIR and contact angle measurements. The flotation experiments have also been carried out and the results showed high recovery percentage of glass beads.

Moreover, silica nanoparticles have been prepared by the Stober method and modified with aminopropyltriethoxy silane (APTS) and mercaptopropyltrimethoxy silane (MPTS) in solvent and aqueous media with post-modification and co-condensation methods. However, flotation results of glass beads when APTS modified silica nanoparticles were employed as collector were not satisfactory which can again related to their hydrophilic characteristics.

Acknowledgement

In the first place, I would like to express my deep appreciation to my advisor Professor Robert H. Pelton for his instruction and constant encouragement during the whole period of my research.

I would like to thank Mr. Doug Keller and Ms. Sally Watson for their assistance with my research. I would like to thank Dr. Bob Berno and Dr. Steve Kornic to help me with Elemental Analysis measurements.

I am grateful to all my colleagues in Interfacial Science and Technologies Group at McMaster: Dr. Anil Khanal, Dr. Wei Chen, Dr. Yuguo Cui, Roozbeh Mafi, Songtao Yang, Kevin Wang, Selina Xu, Dan Zhang, Roger Ren, Leo Hsu, Jack Zhang, Quan Wen, Jerry Li, Tracy Wang, Vincent Leung, Sana Jahanshahi, Hajir Mokhtari, Carla Abarca, Jerry Liu, Bruce Chen and Terry Sato.

I would like to thank my wife Sara Mohajeri for her love, patience and support. I would not be able to succeed without her sacrifice and encouragement. My mother Masoomeh Hessam Mohseni and my father Akbar Naderi Zand, without them and without their inspiration, support and love I would never exist and be who I am. They sacrificed their lives for me to grow up and accomplish. My sisters Bahareh and my brother Reza, for the times being together and their love and encouragement. I dedicate this work to all of them.

Finally, I would like to thank VALE Company and Ontario Center of Excellence for the financial support.

TABLE OF CONTENTS

ABSTRACT ..... **iii**

ACKNOWLEDGEMENT ..... **iv**

TABLE OF CONTENTS ..... **v**

CHAPTER 1 Introduction and Literature Review **1**

1.1 Flotation 2

1.2 History of flotation 3

1.3 Chemistry of flotation 3

1.3.1 Collectors 4

1.3.1.1 Xanthates 4

1.3.1.2 Amines 7

1.3.1.3 Adsorption of collectors onto minerals 7

1.3.2 Other regulating agents in flotation 9

1.4 Problems in flotation 10

1.5 Metal ions and hydroxy species in solution 11

1.6 Electrochemical reactions in solution 12

1.7 The effect of electrical double layer on flotation of minerals 13

1.8 Surface forces in flotation 14

1.8.1 Van der Waals interactions 14

1.8.2 Electrostatic double layer 15

1.8.3 Non-DLVO interactions 15

1.8.4 Extended DLVO theory 15

1.9 Hydrophilicity, hydrophobicity and contact angle 17

1.10 Precipitated calcium carbonate nanoparticle 21

1.11 Silica nanoparticle 23

1.12 References 25

Chapter 2 Preparation and characterization of uniform nickel sulfide thin films on glass for model adhesion studies 29

2.1 Abstract 29

2.2 Introduction 29

2.3 Experimental 30

2.3.1 Materials 30

2.3.2 SILAR deposition 30

2.3.3 Profilometry 31

2.3.4 Atomic Force Microscope (AFM) 31

2.3.5 Scanning Electron Microscopy (SEM) 31

2.4 Results and Discussion 32

2.5 Suggestions for future work 37

2.6 Conclusions 38

2.7 References 39

Chapter 3 First generation inorganic particles as flotation collectors 40

3.1 Abstract 40

3.2 Introduction 40

3.2.1 Precipitated Calcium Carbonate (PCC) 40

3.2.2 Colloidal Silica 41

3.3 Experimental 42

3.3.1 Treatment with stearic acid 42

3.3.2 Dispersion of PCC in water 43

3.3.2 Electrophoresis 43

3.3.3 Dynamic Light Scattering (DLS) 43

3.3.4 Contact Angle measurement 43

3.3.5 Titration 43

3.3.6 Scanning electron microscopy (SEM) 44

3.3.7 Flotation 45

3.4 Results and Discussion 46
3.4.1 Mean particle size and mobility 46
3.4.2 Water contact angle 46
3.4.3 Titration 47
3.4.4 Flotation 48
3.4.5 SEM 49
3.4.6 Experiments for reduction of the particle size 51
3.4.7 Post-hydrophobizing technique 51
3.4.8 Increasing the mobility 51
3.4.9 Colloidal Silica 52
3.5 Conclusion 54
3.6 References 56

Chapter 4 Second generation inorganic particles as flotation collectors 57
4.1 Abstract 57
4.2 Introduction 57
4.2.1 Synthesis of Precipitated Calcium Carbonate (PCC) 57
4.2.2 Modification of colloidal silica nanoparticles with silane coupling agents 58
4.3 Experimental 59
4.3.1 Synthesis of stearic acid treated PCC 59
4.3.2 Synthesis of colloidal silica nanoparticles 60
4.3.3 Preparation of silane-functionalized silica in solvent solution with post-modification method 60
4.3.4 Preparation of silane-functionalized silica in aqueous solution with post-modification method 60
4.3.5 Preparation of silane-functionalized silica in solvent solution with co-condensation method 60
4.3.6 Electrophoresis 61

4.3.7 Dynamic Light Scattering (DLS) 61
4.3.8 Contact Angle measurement 62
4.3.9 Fourier Transform Infrared Spectrometry (FTIR) 62
4.3.10 Si-NMR 62
4.3.11 Flotation 62
4.4 Results and discussion 63
4.4.1 Characterization of PCC nanoparticles 63
4.4.1.1 Mean particle size and mobility of PCC 63
4.4.1.2 FTIR experiments of PCC samples 63
4.4.1.3 Water contact angle 64
4.4.1.4 Flotation by employing PCC nanoparticles 65
4.4.2 Characterization of silica nanoparticles 65
4.4.2.1 Mean particle size and mobility of silica nanoparticles 65
4.4.2.2 Solid state ^{29}Si NMR 66
4.4.2.3 Mean particle size and mobility of silane-functionalized silica in solvent solution with post-modification method 67
4.4.2.4 Mean particle size and mobility of silane-functionalized silica in aqueous solution with post-modification method 67
4.4.2.5 Mean particle size and mobility of silane-functionalized silica in solvent solution with co-condensation method 68
4.4.2.6 FTIR experiments on silica and silane treated silica nanoparticles 68
4.4.2.7 Flotation by employing amino silane functionalized silica nanoparticle 69
4.5 Conclusion 70
4.6 References 70

Chapter 1

Introduction and Literature Review

The technology of froth flotation was first invented for the concentrates of sulfide minerals[1]. Since then it has been employed for lots of other mineral and non-mineral applications such as separation of energy minerals like coal and bitumen[2], waste water treatment[3], and deinking of recycled papers[4] and resource recovery from industrial wastes[5].

Flotation is generally based on physical phenomena occurring at solid/water/air interfaces. Therefore, surface chemistry principles are very important factors in flotation technology. Having knowledge about aqueous solution chemistry and electrochemistry helps us to have a better in sight about the reactions in flotation systems[6].

The goal of my work was to synthesize an appropriate inorganic nanoparticle as a collector for flotation of glass beads and also to prepare thin film of nickel sulfide. The first step was preparing a very uniform thin layer of nickel sulfide for model adhesion studies. The method employed was successive ionic layer adsorption and reaction (SILAR), which was based on adsorption of a cationic precursor and reaction with anionic precursor. The profilometry, AFM and SEM results show a weak deposited layer of nickel sulfide on glass, which was very uneven at low SILAR deposition cycles and very porous at high SILAR deposition cycles.

In the next step, commercial grades of precipitated calcium carbonate (PCC) and colloidal silica were prepared and employed as collector for flotation of glass beads. Also, stearic acid treatments were carried out on untreated PCC samples. Despite that the mean particle size of PCC particles are in the nano range, they aggregated in aqueous solution and particle size increased to micron range.

Therefore, deposition of these particles to glass beads was very low and consequently flotation results were not satisfactory. SEM images confirmed low deposition of PCC particles to glass beads. A wide range of methods have been tried to decrease the particle size of PCC particles but none of them were successful.

In another series of experiments, colloidal silica was employed as a collector for flotation of glass beads. These particles have colloidal stability at pH 4 but they aggregated when the pH was increased to 9 which is the flotation operating pH. These particles did not show good deposition to glass beads or good flotation ability from pH 4 to 9. The reasons could be hydrophilicity of colloidal silica at low pH and their aggregation at high pH.

Also, stearic acid treated PCC nanoparticles were synthesized with a carbonation method and characterized with electrophoretic mobility, dynamic light scattering, FTIR and contact angle measurements. The flotation experiments were also carried out by employing PCC nanoparticles and the results showed high recovery percentage of glass beads.

Moreover, silica nanoparticles have been prepared by the Stober method. Furthermore, they have been modified with aminopropyltriethoxy silane (APTS) and mercaptopropyltrimethoxy silane (MPTS) in solvent and also aqueous media with post-modification and co-condensation methods. Characterization experiments confirmed synthesis of silane modified nano silica particles.

However, flotation results of glass beads when APTS modified silica nanoparticles were employed as collector are not very satisfactory which can be related to their hydrophilic characteristics.

In the following sections, background information about the chemistry and electrochemistry of flotation and the interaction of inorganic nanoparticles as collector with glass beads will be introduced.

1.1 Flotation

From the first decade of the 20th century, flotation became the main method for mineral separation[1]. The main reasons for this predomination are high efficient treatment of lower-grade ores, the broad application of process with respect to particle size, with almost no limitations in separating different minerals with different surface chemistries [7].

Flotation or more formally froth flotation is by far the most common of the separation processes. In fact, froth flotation is a key interfacial technology to recover minerals from sulfides and oxide minerals to water soluble minerals such as potash (KCl) and energy minerals (coal and tar sands)[8,9].

This versatility has led to applications outside of the mineral industry as a separation means for hydrophobic materials, such as de-inking recycled papers and in the area of wastewater treatment [10, 11].

In all these applications, the separated targets should be hydrophobic enough for the attachment by air bubbles. If they are not sufficiently hydrophobic, surface active compounds called mineral collectors are usually added to enhance the surface hydrophobicity [12]. Despite that collectors are the most important reagents used in the flotation, it is clear that lots of other regulating agents should be used in this separation process which is divided into six main groups: pH modifiers, depressants, activators, frothers, coagulants and flocculants [13].

But, before explaining about the chemistry of flotation, first, the history of flotation has been studied. In fact, flotation is one of the major technologies which helped human being by opening previously un-treatable minerals and providing cheap natural resources.

1.2 History of flotation

The history of flotation process goes back to a British Patent issued to W. Haynes in 1860. The original observation was when oil from gravity processing machinery accidentally mixed with ores and sulfides showed different wetting characteristics from gangue minerals. Thus, he based his process on the mixing of dry ore with oil and then with water and separating oil-wetted sulfide minerals from water-wetted gangue.
Francis and Alexander Elmores modified this process (US Patent in 1900 and 1901) and called it the bulk oil flotation process but the consumption of oil was high and ore and oil often mixed in equal parts.

In 1902, operators at Broken Hill, Australia discovered that a considerable amount of the lead and zinc minerals floated on the froth produced by violent mixing in the presence of air. Thus, the importance of gas bubbles was recognized and patented on bubble generation techniques by Potter (1901), Cattermole and Delpart (1902), and Francis Elmore (1904). These methods were based on mixing acid and carbonate rock to generate CO_2 gas bubbles. In this way, the amount of oil used was decreased.

But, Minerals Separation Ltd. was the pioneer of the modern flotation process which reduced the oil content to less than 1% and agitated the ore slurry. In this method, the bubbles would rise to the top of the froth. This process was first installed at Broken Hill in Australia in 1905.

Flotation became established as a technology around 1910, first in Australia and followed rapidly in the US and a little later in Canada. But, there appear to have been several failures especially for separation, also; the process did not work on some ores. So, the subsequent developments were done to extend the process in order to introduce differential flotation to separate two or more minerals especially sulfhides from each other. The important developments are as follow[14]:

- Introducing soluble frothing agents such as alcohols (1908)
- Utilizing alkaline pH to float and depress sulfides (1910)
- Developing different kinds of depressants and reactive agents (1913)
- Manufacturing collectors (1922)
- Introducing xanthates as dominant collectors in flotation (1925)

1.3 Chemistry of flotation

As indicated above, the process of separating one mineral from other minerals in flotation process depends on how easy a particle becomes wetted by water (hydrophilicity) and which one likes the bubbles more (hydrophobicity). Since most minerals are hydrophilic, the surface must be treated with chemicals called collectors[15]. Here, the chemistry and mechanism of collectors in flotation systems will be explained.

1.3.1 Collectors

The general composition of a collector is a hydrocarbon chain with a reactive or functional head group. The head group reacts with the surface of the mineral and the hydrocarbon group (or tail) is oriented away from the surface towards the water. Therefore, when the collector adsorbs onto the mineral surface its characteristic converts from hydrophilic to hydrophobic[16]. Figure 1.1 shows the general concept of attachment of a collector to a mineral surface.

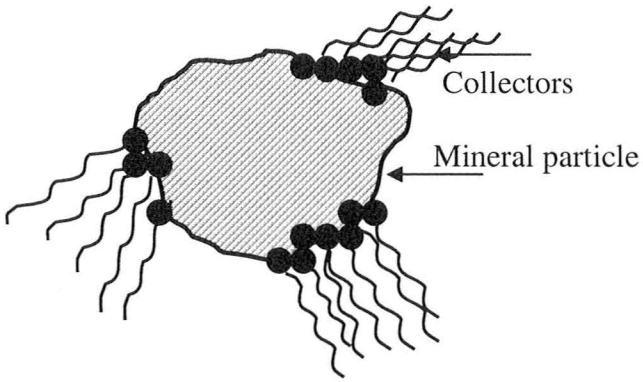

Figure 1.1 Schematic illustration of attachment and orientation of a collector to a mineral particle

As mentioned above, collector is the most important chemical in mineral flotation. Therefore, selection of collector is certainly very critical for floated and rejected minerals. The chemistry and reactions of thiols and amines are examples of the two most important collectors in flotation systems and are described here.

1.3.1.1 Xanthates

Thiol or sulfhydryls collectors are type of collectors which are used a lot for sulfide mineral flotation. There are large numbers of compounds that are employed as thiol collectors which are listed in table 1.1.

Mercaptans:

Mercaptans have a very poor solubility in water. The major advantage of the mercaptans is their ability to collect base metal oxide minerals which are always found in sulfide deposits. In some sites, mercaptans are used as auxiliary collectors[17].

Xanthates:

Xanthates are the most common class of collectors used for sulfide minerals. They are mostly used in potassium amyl, sodium ethyl, sodium isopropyl, and sodium butyl forms. Xanthates are prepared by reaction of an alcohol with carbon disulfide in alkaline solution as shown bellow:

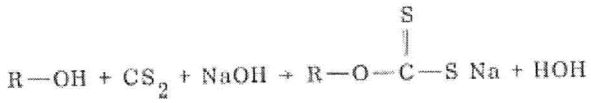

The alcohol normally contains two to six carbons and may be the normal, iso, or secondary form. If mercaptan is used instead of alcohol, we would have trithiocarbonate. Xanthates are strong collectors with reasonable water solubility, good stability in alkaline solution, relatively low cost, with easy of manufacturing, transport, storage and handling[15]. The alkali metal salts ($ROCS_2Na$) and acid ($ROCS_2H$) molecules are unstable in water and in aqueous media the salt ionizes completely to give negatively charged xanthate ions as illustrated bellow:

In strongly acid solutions, xanthate decomposes to its components very quickly at pH 2-3[15]. The reactive head group is CS_2^- and the name of xanthate is given from the R group. The common xanthates are ethyl xanthate and amyl xanthate which structurally are depicted in Figure 1.2.

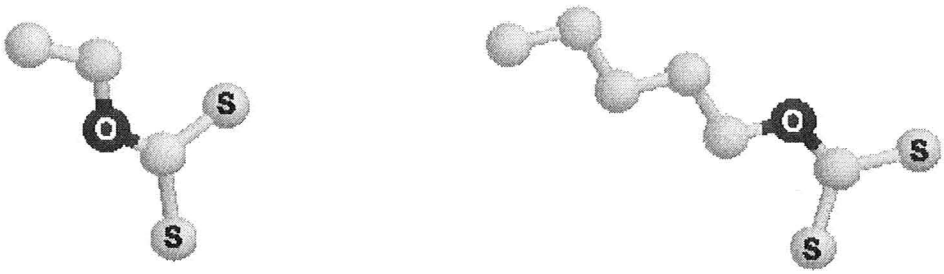

Figure1.2 Structure of ethyl xanthate (left) and amyl xanthate (right)

Xanthogen formates:

The xanthogen formates are manufactured by reacting xanthates with alkyl chloroformates in solution as follow:

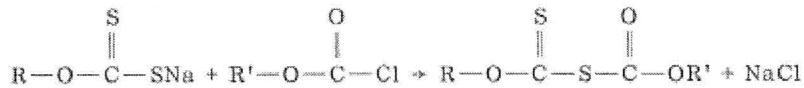

These collectors are very common collectors for copper sulfides.

Xanthic esters:

Xanthic esters have the general formula ROC(S)SR and are prepared by reacting a xanthate with an alkyl chloride as follows:

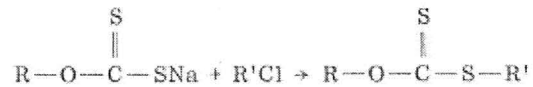

They are good collectors for metallic copper, molybdenite, and sulfidized base metal oxides and are effective in both acid and alkaline solutions.

Table 1.1 Common thiol collectors

Collector type	Formula
Mercaptan	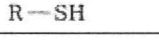
Dithiocarbonate (xanthate)	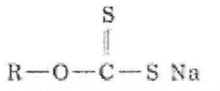
Trithiocarbonate	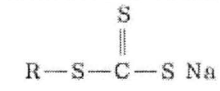
Xanthogen formate	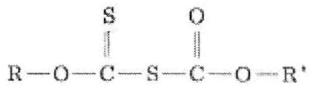
Xanthic ester	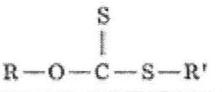
Dithiophosphate	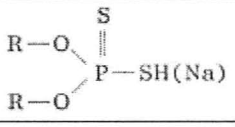
Thionocarbamate	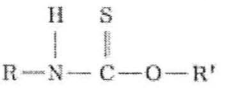

Dithiophosphate:

Dithiophosphates are prepared in the same preparation methods of xanthates; just P_2O_5 is used instead of CS_2 as follow:

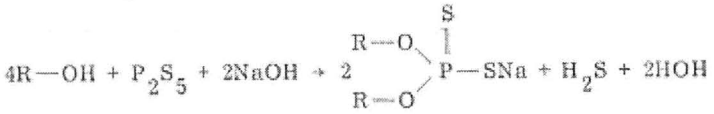

Thiocarbamate:

The thiocarbamates are only a little soluble in water. These collectors are made by the reaction of a xanthate with methyl chloride and the reaction of the product with an amine as follow:

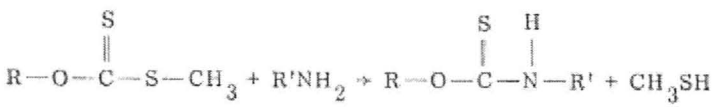

They are stable in acidic situations and can be used in a wide pH range [18, 19].

1.3.1.2 Amines

Amines are usually used in the flotation of non-sulfide minerals, for instance separation of silica from iron oxides[20]. Amines are supplied as chloride or acetate salts. The most common amine collector is dodecylammonium hydrochloride (RNH_3Cl) which is usually called dodecylammonium. This collector ionizes in water to give the cationic collector (RNH_3^+) where NH_3^+ is the head. It is obvious that these collectors are pH sensitive[21].

1.3.1.3 Adsorption of collectors onto minerals

The adsorption mechanism of collectors to mineral surfaces can be divided into two major categories: chemical adsorption (chemisorption) and physical adsorption (physisorption). Adsorption of xanthate on a sulfide is an example of chemisorption [22].

To explain about chemisorption, the reaction between xanthate and galena (PbS) is illustrated here. Xanthate can react with galena in two ways: ion exchange, and electron transfer[23] to form Pb-X bond.

In ion exchange, xanthate which is an anion can exchange its ions with other anions which are hydroxide (OH^-) and sulfide ($SO4^{2-}$) (the oxidation reaction products). Since these oxidation products are hydrophilic, these ion exchanges with xanthate significantly enhance the hydrophobic characteristics of galena and its attachment to air bubbles[24].

Electron exchange reaction involves one species losing an electron (oxidized) and another gaining an electron (reduced). Again, the reaction between xanthate and galena is provides an example. In this case, xanthate is oxidized and the electron moves through the galena to an oxygen. The oxygen accepts the electron and is reduced to hydroxyl (OH^-)[24]. The electron transfer process is depicted schematically in Figure 1.3.

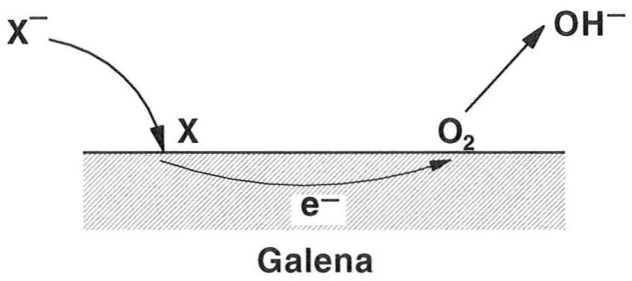

Figure1.3 Electron transfer from xanthate to oxygen via the surface of galena[24]

On the other hand, adsorption of amine onto silica is an instance of physisortion. In the case of physical adsorption a covalent chemical bond does not form and the origin of the adsorption mechanism is based on the fact that most solid particles in water have a charge on their surface as surface charge. In the case of adsorption amine onto silica, an

amine which is positively charged is attracted and adsorbed electrostatically to negatively charged silica. It should mention that pH and ionic strength of solution play very important roles here[25].

Also, there are considerable differences in the relative energies of adsorption. With heterogeneous solid surfaces, localized chemisorption takes place on active sites like kinks and ledges, emerging dislocations and lattice defects. High energy of adsorption may lead to a perturbation of the surfaces and definite distortion and may even break the chemical bonds between the atomic species constituting the adsorption site and the rest of the solid. This type of bond breakage differs from a true desorption[26].

It is well known that every surfactant cannot act as a collector for a given solid. A surfactant that converts a hydrophilic surface to a hydrophobic one must be adsorbed in a way that it is relatively immobilized. This immobilization denotes the ability to withstand movement of the liquid along the shear plane adjacent to the solid without displacement. Otherwise, a complete wetting of the solid would ensure. The concept of relative immobilization of collector molecules imposes a condition such that of the various adsorption states. Only the states within the intermediate energy levels may be appropriate for flotation purpose.

A very strong adsorption may lead to an excessive weakening or even a breakage of residual bonds between the adsorption site and the solid. Some species, either physically adsorbed or chemically adsorbed may be too weakly adsorbed to withstand the external forces imposed during attachment bubbles. The immobilization implies that the energy for translation from one adsorption site to another is of appropriate value[15].

In this situation, a nonpolar molecule may become relatively immobilized when a sufficient number of $-CH_2-$ groups of this molecule develop multiple van der Waals bonds with a nonpolar substrate. Also, development of any bonds, whether van der Waals bonds between hydrocarbon chains or hydrogen bonds between the hydrated polar groups or hydroxylated counterions may lead to immobilization of the adsorbate species[27].

Based on the differences in properties of surfactants, their adsorption may be discussed relative to their classification, or relative to the group of solids being floated. However, because of the complexity of flotation systems, no classification approach is sufficiently appropriate[28].

The following requirements should be considered for a surfactant to act as a collector:

1. Relative immobilization of the surfactant species (as discussed above)
2. Sufficiently hydrophobic character to be floated and suffer the mechanical and dynamic effects of a flotation system.
3. Selectivity at appropriate pH that would permit high recovery and purity.
4. Suitable choice of a collector-frother combination that would permit satisfactory kinetics of separation to be achieved.

The first two requirements are basic for the selection of an appropriate collector. They impose conditions on the polar groups which develop bonding with the solid and on the nonpolar groups that regulate subsequent development of hydrophobicity. These two requirements may be met by selecting a surfactant species incorporating appropriate polar and nonpolar groups or by a choice of two species, one fulfilling the requirement of

developing the primary bond with the substrate and the other producing a sufficient degree of hydrophobicity by secondary (mostly van der Waals) bonding.

Requirement 3 determines which of the available modifiers can be used to improve selectivity; if no suitable modifiers can be found, the surfactant is not a useful collector, however successfully it meets the first two requirements. Similarly, as regards requirement 4, if a collector causes such hydrophobicity that solid particles aggregate and no appropriate frother can be found to foster their attachment to air bubbles, that reagent is also not a suitable collector[28].

1.3.2 Other regulating agents in flotation

As described above, the adsorption mechanisms either chemisorption or physisorption are pH dependent. One of the most important properties of a particle is its point of zero charge (pzc) where the surface charge of particle becomes zero. PZC is an important property because the particle is positively charged at pH<pzc and negatively charged at pH>pzc[29].

The most common pH modifier in sulfide flotation systems is soda ash (sodium carbonate, Na_2CO_3) because of its dual effect. The maximum pH obtained with soda ash is about 10. Carbonate ions will charge the pH and also can form insoluble precipitates with dissolved or adsorbed metal ions such as calcium. Due to the excess addition of carbonate ions, conversion of all detrimental calcium ions to calcium carbonate would be guaranteed. Calcium carbonate is highly insoluble and forms a precipitate which could help the displacement of adsorbed calcium on the sulfide mineral surface[30].

The other component in flotation systems is a depressant. A depressant is a reagent that causes a mineral to cease to float which in the absence of the reagent, the mineral would float. Depressants function by a variety of mechanisms such as reacting with mineral surface to form a hydrophilic site, reacting to form compounds that block or slow down collector adsorption, removing or cleaning species from surface that react with collectors, making conditions more retarding xanthate adsorption, making conditions more oxidizing to promote formation of hydrophilic oxidation products on a sulfide mineral, removing oxygen to retard xanthate adsorption, and destroying hydrophobic species on the mineral surface[31, 32].

On the other hand, an activator is a reagent which causes a mineral to float with a collector which otherwise would not. Some sulfides such as Sphalerite ((Zn,Fe)S) does not adsorb to collectors very well and Zinc- Xanthate is not stable. In these situations, a collector should be employed to enhance the adsorption of the collector to the mineral. The most important activator in this system is $CuSO_4$. The activation mechanism is exchanging Cu^{2+} ion with Zn^{2+} ion that the mineral surface takes on some characters of copper sulfide which react with xanthate faster[33].

$$ZnS_{(S)} + Cu^{2+}{}_{(aq)} \longrightarrow CuS_{(S)} + Zn^{2+}{}_{(aq)}$$

Frothers preserve the small bubbles produced in the flotation cell and enable the formation a stable froth on the surface of the slurry by adsorbing on the bubbles and modifying the surface properties of them.

The simplest frothers are alcohols which accumulate at the surface of the bubble with the hydrocarbon chain on the air side and the OH group on the water side. In the absence of frothers, bubbles rapidly coalesce into the larger bubbles which are detrimental to particle collection and froth stability[34]. Typical current frothers are methylisobutylcarbinol (MIBC), the Dowfroth series based on polypropylene glycol methyl ether, and 1, 1, 3 triethoxybutane (TEB).

Coagulating agents (coagulants) and flocculating agents (flocculants) do the reverse action of dispersants and cause the particles to aggregate. This is detrimental for flotation unless selective agglomeration can be achieved. Furthermore, distinction between two or more types of minerals (selectivity) is very important in agglomeration mechanism.

Coagulants function by bringing the surface charge close to zero or by reducing the double layers. Metal ions are some examples of strong coagulants because of their positive charge. Also, increasing the electrolyte can decrease the electrostatic repulsive forces between fine charged particles[35].

Flocculants are long chain organic reagents with reactive head groups along the length of the chain. Polymers should be long enough to adsorb on several particles simultaneously and thus cause them to aggregate[36, 37].

1.4 Problems in flotation

There are some difficulties in flotation process which can be concluded as below:

- An extensive surface oxidation of sulfide minerals
- The existence of other minerals such as oxides, carbonates, and sulfates with sulfides
- The coexistence of valuable sulfides and non-sulfides with the hydrophobic minerals such as talc, graphite, and molybdenite
- Interlocking of valuable fine particles within massive amounts of gangue minerals

It is obvious that if we want to have an efficient separation, all of the above problems should be analyzed and dealt separately[38].

Extensive oxidation of sulfides could be canceled out with appropriate amounts of HS^- to convert the oxidized layer to suitable sulfides. In the case of coexistence of sulfides with the oxidized minerals, the sequence of flotation steps would be employed. In this method, first the sulfides are floated and then a separation of the oxidized minerals using suitable activators and/or appropriate collectors is carried out[39].

The existence of even minor quantities of naturally hydrophobic minerals in an ore makes the separation process more difficult. Therefore, before adding any collector to the system employing an appropriate depressant is essential to depress flotation of undesirable minerals. But, sometimes softness of these hydrophobic minerals makes some

problems during grinding. They become smeared on other particles. When such smearing occurs, the use of depressants is not capable of providing a sufficient degree of selectivity especially whenever extensive grinding is needed. Sometimes, introducing depressant to the grinding circuit and pulp density reduction in the mills is helpful to reduce the smearing effect.

Interlocking of the valuable minerals with gangue minerals is an important problem for efficient separation in flotation process. The problem would be even worse if the valuable and gangue minerals have a very similar chemical composition and the valuable minerals are very fine. Laboratory and in-plant investigations established that the very coarse and the very fine size particles do not float very well[40].

Many experiments have been done and numerous solutions have been offered for this problem. The influence of particle size on the rate of recovery of minerals has been investigated since 1931. In general, fine and ultrafine particles have low collision efficiencies with bubbles and are accessible to mechanical entrainment. Moreover, due to the small mass and large specific surface area of fine particles problems such as high reagent consumption, non-selectivity of the collector, excess froth stability, mechanical entrainment of fine particles, etc., affect the recovery and grade of the floated product[41, 42].

On the other hand, size range for more efficient recovery depends on mineral type and is based on the attachment, adhesion, and stability of mineral particles with air bubbles. For example the size ranges for maximum recovery in some cases are: galena (PbS) (6- 70 μm), sphalerite ((Zn,Fe)S) (8- 90 μm), pyrrhotite (FeS) (9, 40 μm), chalcopyrite ((Cu,Fe)S_2) (15- 60 μm), arsenopyrite ((Fe,As)S) (15- 120 μm) and pyrite (FeS_2) (20- 150 μm). Bellow the minimum (fine) and above the maximum (coarse) sizes the flotation recoveries start to decrease[43].

In approach for the fine particle flotation, we can say that the fundamental reason for low flotation rate of these particles is due to their low collision efficiency with flotation bubbles[44]. Lots of experiments have been done during these years to increase bubble- particle collision efficiency by decreasing bubble size or increasing mineral particle size.

The poor recovery in flotation of coarse particles is also explained by the inability of bubbles to carry large particles to the top of the flotation cell. Also, under high agitation the centrifugal forces overcome and separate large particles from fine particles and bubbles[45, 46].

1.5 Metal ions and hydroxy species in solution

When a metal salt is dissolved in water in a flotation bath, it dissociates into the cation M^+ and anion A^- . The extent of hydrolysis depends on the pH of water. The general reaction can be represented as below:

$$M^+ + OH^- + H^+ + A^- \leftrightarrow M^+ + A^- + H_2O$$

If the metal hydroxide and the acid are both strongly dissociated, the neutralization is largely irreversible like neutralization of a strong base with a strong acid. But, if the metal hydroxide is not strongly dissociated, the reverse reaction occurs and equilibrium is reached[47].

As the pH is increased the metal ion first forms a metal hydroxy species and metal hydroxide with more increasing of pH. This is illustrated by iron as below:

$$Fe^{3+} + H_2O \leftrightarrow Fe(OH)^{2+} + H^+$$

$$Fe(OH)^{2+} + H_2O \leftrightarrow Fe(OH)_2^{+} + H^+$$

$$Fe(OH)_2^{+} + H_2O \leftrightarrow Fe(OH)_3 + H^+$$

Metal ion and metal hydroxy species play a significant role in flotation. They influence the collector action by interacting with the collector and also alter the mineral surface charge by electrostatic adsorption[48, 49].

1.6 Electrochemical reactions in solution

Electrochemical reactions are a large class of chemical reactions where a molecule species is oxidized and another one is reduced simultaneously. They are also called redox or charge transfer reactions. In the overall reaction, the electron is transferred from a species which is oxidized to the one which is reduced[50].

These kinds of reactions are very important in flotation of sulfide minerals and are the result of the chemical reactivity of sulfur with different oxidation states. The chemical reactivity of sulfur and its variable oxidation state leads to charge transfer reactions of sulfide minerals in water. The oxidation reaction for a sulfide mineral in water can be represented as below[51]:

$$MS + xH_2O \longrightarrow M(H_2O)_x^{2+} + S^- + e$$

$$M(H_2O)_x^{2+} \longrightarrow M(OH)(H_2O)_y^{+} + H^+ + (x\text{-}y\text{-}1)H_2O$$

$$M(OH)(H_2O)_y^{+} \longrightarrow M(OH)_2.zH2O + H^+ + (y\text{-}z\text{-}1)H_2O$$

Where M is a bivalent ion and S^- is an intermediate product in the oxidation. The hydroxyl species formed by hydrolysis play a significant role in some of the flotation processes[51].

1.7 The effect of electrical double layer on flotation of minerals

A solid surface in water bears a uniform charge density which develops a potential at the surface. Most mineral flotation systems have different charged species. When a mineral is introduced in water, a water/solid interface is created. Indeed, any change in the sign and magnitude of surface charge affects the collector interaction[52]. Figure 1.4 depicts a schematic electric double layer which is commonly applied in many areas of surface chemistry of flotation. It shows counter ions and the potential drop across the double layer[53].

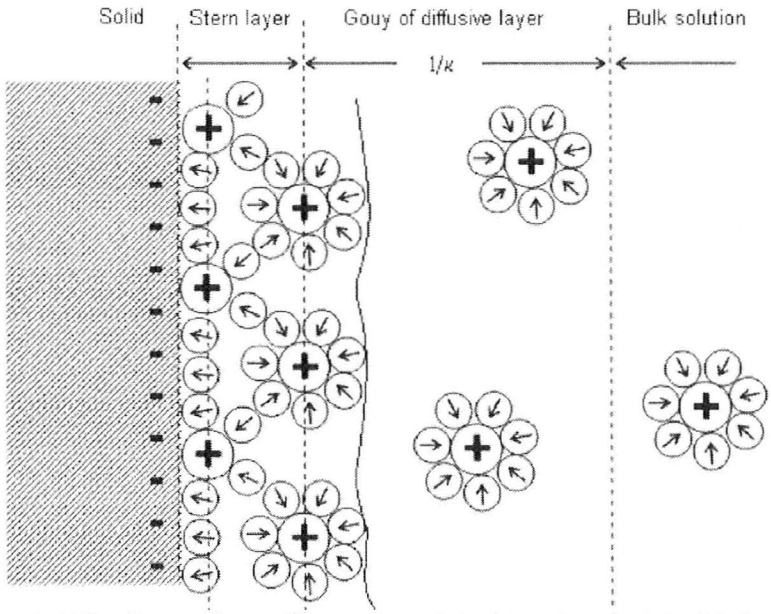

Figure1.4 The Stern- Gouy- Chapman model of the electrical double layer[53]

Most mineral flotation systems are composed of charged species. When minerals are suspended in water a solid/water interface is created. Charged species are transferred across the interface until the water becomes saturated with the ions derived from solid. This ion transfer continued until equilibrium is achieved.

Ions from solids and those which travel across the interface control the double layer potential. As long as the potential of these ions is constant, equilibrium is reached. The ions which pass between the two phases and establish the electric double layer are known as potential determining ions. The concentration of these ions in the aqueous phase determines the magnitude and sign of the zeta potential[54].

In addition to the potential determining ions, other ions which exist in the solution can function as counter ions. These ions are adsorbed by electrostatic attraction only and can affect the magnitude of the zeta potential. In order to reduce the effect of these ions

on zeta potential a background electrolyte is used in the measurement of zeta potential. It brings constant ionic strength to measure the zeta potential changes caused by adsorption at the surface.

Different electrolytes do not change the surface charges as they do not pass between solution and solids. But, they can change the zeta potential as they occur in the diffuse layer. At high concentration electrolytes the double layer collapses and zeta potential does not exist despite that the surface of mineral is still charged which is called double layer compression[55].

The effect of these ions on zeta potential is minimized by measuring in a background electrolyte which will bring a constant ionic strength. Therefore, the variations in zeta potential just are caused by the adsorbing ions which are of interest in determining the adsorption of collectors in flotation.

In the flotation of sulfide minerals when two minerals have opposite surface charge, selectivity is affected adversely. An example of this is found in the flotation of pentlandite from serpentinite ores. With as little as 10% serpentine, the recovery of pentlandite is reduced from over 90% to below 80% and with 30% serpentine in the feed, it is reduced to less than 25%. The main cause is surface charge. The pentlandite particles are negatively charged at pH> 4 in presence of xanthate. On the other hand, the serpentine particles are positively charged up to pH 9. In this way, adding carboxy methyl cellulose dispersant can reduce the negative value of serpentine's surface charge[56].

1.8 Surface forces in flotation

An intervening liquid film is formed between a particle and a bubble when the particle and the bubble are in close proximity. This film is normally stable between hydrophilic surfaces, whereas it is usually unstable between a hydrophobic particle and an air bubble. The stability of the intervening liquid film can be understood using surface force concepts. Here, the surface forces are divided into three interactions:

- Van der Waals
- Electrical double layer
- Non-DLVO

The first two interactions are together referred to as DLVO interactions.

1.8.1 Van der Waals interactions

Van der Waals forces are universal forces between atoms and molecules. These forces also operate between macroscopic objects like bubbles and particles. The interaction between macroscopic bodies arises from spontaneous electric and magnetic polarizations, which give rise to a fluctuating electromagnetic field within the media and the gap between them[53]. To calculate the van der Waals interactions between a particle and bubble, the Hamaker constant is negative, which results in a repulsive van der Waals interaction[57, 58].

1.8.2 Electrostatic double layer

As mentioned before, air bubbles and mineral particles are charged in aqueous media for various possible reasons, such as the ionization of surface groups, specific adsorption of ions, preferential solubility of surface ions and several others. In an electrolyte solution, the distribution of oppositely charged counter ions is accumulated around the charged particles to balance the surface charge. These counter ions are for electrostatic attraction trying to move the counter ions close to the particle/bubble surface[59].

When a charged bubble and a charged particle come close to each other, their diffuse layers overlap and they start to interact. The electrostatic double layer interaction is mainly dependent on the surface potential and the extent of the diffuse layer.

It is reasonable that the electrostatic double layer interaction energies are repulsive (positive) with surface potentials of like sign and attractive (negative) with surface potentials of unlike sign at large surface separation distances.

However, at small surface separation distances charge reversal may occur and the electrostatic double layer interaction energy may be attractive with surface potentials of like sign but unequal magnitude and repulsive with surface potentials of opposite sign[60].

1.8.3 Non-DLVO interactions

The most significant non-DLVO forces which can affect bubble–particle attachment are hydration forces, hydrophobic forces and steric forces. The presence of solid or gas at the surface significantly disturbs the structure of water adjacent to the surface. Overlapping of the disturbed water molecules requires work to be done which leads to repulsive hydration forces for hydrophilic surfaces and attractive hydrophobic forces for hydrophobic surfaces.

Steric forces arise from macromolecular reagents which are adsorbed on particles and bubbles. The steric interaction is mainly repulsive in flotation, and these reagents are often considered to be depressants[61].

Also, the presence of very small bubbles on the surface of a particle can lead to an attraction that appears to be similar to the action of hydrophobic forces. The base of the effect is the change in the magnitude and the sign of the van der Waals interactions between a particle and a macrobubble. This interaction is repulsive, but as particle surface hydrophobicity increases, the number, size and height of nucleated nanobubbles increase, resulting in an attractive interaction[62, 63].

1.8.4 Extended DLVO theory

In the classical DLVO theory, the total interaction energy is the sum of the van der Waals and electrostatic double layer energies:

$$V_{DLVO}(H) = V_{vdw}(H) + V_e(H)$$

But, in the extended DLVO theory, the hydrophobic interaction energy is included[64]:

$$V_{DLVO}(H) = V_{vdw}(H) + V_e(H) + V_h(H)$$

For attachment between a bubble and a hydrophobic negatively charged particle the van der Waals and the electrostatic double layer interaction energies are repulsive and the hydrophobic interaction energy is attractive. As shown in Fig. 5, the repulsion outweighs the attraction causing a potential energy barrier. For bubble–particle attachment, the particle needs to have sufficient energy to overcome this energy barrier. If the particle overcomes the energy barrier, we have dewetting in primary minimum, the thin film between the particle and the bubble ruptures and a three-phase contact line is formed.

Another feature in Fig. 1.5 is a secondary minimum, which happens for different distance dependencies of the van der Waals, electrostatic double layer and hydrophobic interaction energies. The depth of the secondary minimum is usually small and therefore particles rarely form stable aggregates with bubbles.

To improve the chance of bubble–particle attachment, the height of the energy barrier has to be decreased. We can do that in different ways. For example, we can decrease the electrostatic double layer repulsion by increasing the ionic strength, or increase the hydrophobic attraction by increasing particle surface hydrophobicity (using collectors). Generally, the van der Waals interaction energy cannot be changed unless the temperature is changed or surface nanobubbles are prepared[65].

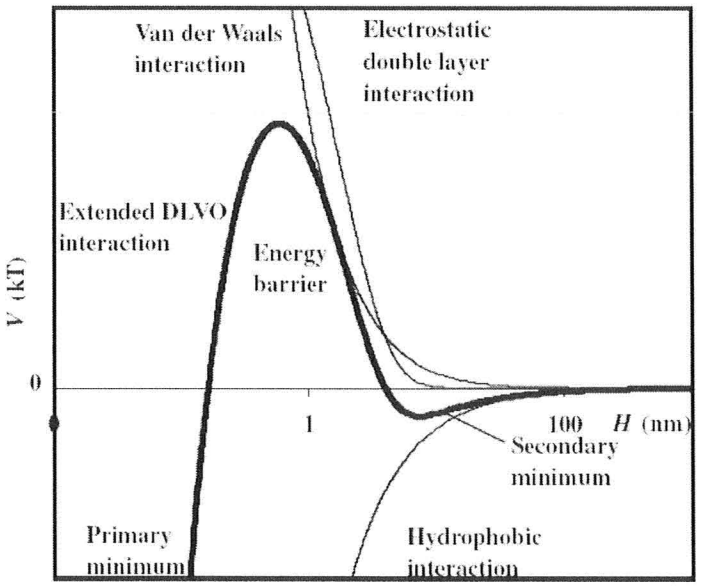

Figure1.5 Potential energy diagram for the interaction of a bubble and a hydrophobic particle as a function of surface-to-surface distance[65]

1.9 Hydrophilicity, hydrophobicity and contact angle

As mentioned above, flotation is based on attachment of the mineral particle to an air bubble. As mineral particles are suspended in water the air bubbles has to displace water from the surface of the mineral and make an effective contact, which occurs when the mineral surface is or has been made hydrophobic to an appreciable degree. Therefore, the concepts of hydrophilicity and hydrophobicity are very important in flotation process. Whether a substrate is wetted with water or not, depends on the structure of its components and their interactions with water. Therefore, understanding the relevant properties of water and considering the bonds between oxygen and hydrogen is very important. Hydrogen and oxygen have a covalent bond with sharing electron. However, the oxygen has higher electronegativity and has a higher attraction to electrons than hydrogen which results a slightly charge separation. It means that the electrons spend more time around the oxygen than around the hydrogen atom. This charge imbalance in water molecules manages the interaction of water with other substances [66].

As an example, consider the straight chain of alcohols: R-OH where R refers to the hydrocarbon chain (C_nH_{2n+1}). Since C and H have similar electronegativities, no substantial charge separation occurs and consequently the R group is non polar. The hydroxyl group (OH), on the other hand, is a polar group. Therefore, water molecules can interact with the OH part of the alcohol as depicted in Figure 1.6.

Figure1.6 The arrangement of electrons around oxygen and hydrogen in a water molecule and with alcoholic OH group

Electrostatic attraction between the δ^- charge on the oxygen of one molecule (or group) interacts with the δ^+ charge on the hydrogen of another group giving rise to a so-called hydrogen bond. This interaction with water means the group is hydrophilic. The non polar R group, having no such ability to interact with water, is hydrophobic [67].

The overall property of the alcohol - hydrophilic or hydrophobic - depends on the relative proportion of R to OH. For example, short hydrocarbon chains such as CH_3 (methyl) and C_2H_5 (ethyl) (i.e., n =1 and 2 in the general formula, respectively) the OH dominates and these alcohols are hydrophilic. This shows in their complete miscibility with water at all concentrations (i.e., their solubility in water is infinite). As the chain lengthens, the hydrophobic character of the R group increasingly dominates and the alcohol becomes less soluble. For example, for n = 8 (octyl alcohol) solubility is down to 0.05 g/g water [68].

For example, surface of a graphite particle is very hydrophobic and the main reason is the existence of C atoms which have no tendency to H-bond with water molecules. On the other hand, silica (SiO_2) surfaces contain oxygen atoms which make

from H-bond with water and make silica hydrophilic. Graphite and silica represent extremes, strongly hydrophobic to strongly hydrophilic properties respectively. Sulfide mineral surfaces lie between these two extremes. Sulphur, on the other hand, is hydrophobic but the surface is usually contaminated by OH and S-O compounds (e.g., SO_4^{2-},) due to the reaction with oxygen and water. These chemicals are hydrophilic because of the presence of oxygen. Like the case of the alcohol molecule, the overall wetting character depends on the balance of hydrophilic and hydrophobic components and generally sulfides are hydrophilic[69].

A measure of hydrophobicity of the mineral particle is the extent to which the air bubble displaces water for the solid surface. This can be understood from an analysis of thermodynamic aspects of the bubble mineral contact.

Air-mineral contact occurs when water is displaced from the solid surface. For this to occur, there must be a finite contact angle at the three phase (air, water, and solid) contact. When the bubble contacts either a solid or a liquid substrate, it minimizes its free energy, first noted by Gibbs. This is expressed by $\gamma_{a/l}A_{a/l} + \gamma_{a/s}A_{a/s} + \gamma_{s/l}A_{s/l}$ which must be minimized, where γ is a surface or interfacial tension, A is area and a/l, a/s and s/l denote respective interfaces between liquid (water), air and solid phases. The decrease in the interfacial area is represented by

$$\Delta A = \Delta A_{a/s} - \Delta A_{s/l} - \Delta A_{a/l}$$

The corresponding free energy change is given by

$$\Delta G_a = \gamma_{a/s}\Delta A_{a/s} - \gamma_{s/l}\Delta A_{s/l} - \gamma_{a/l}\Delta A_{a/l}$$

If ΔG_a is negative, the process of air-mineral contact is spontaneous[70].

The attachment of a particle to an air bubble in water is shown schematically in Figure 1.7. The contact angle is the angle between planes tangent to the surface of the solid and the liquid at the wetting perimeter. In air-mineral-water system it is measured through the gas (air) phase. The wetting perimeter is a small zone where the three phases merge and is referred to as the three-phase line of contact (tplc) [71].

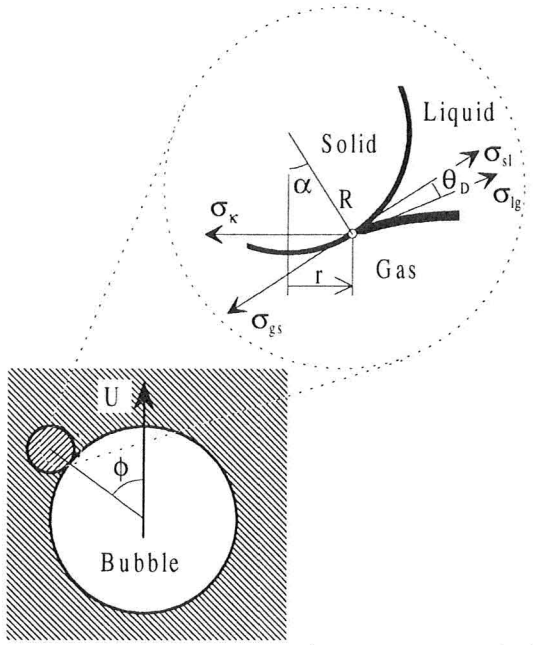

Figure1.7 Three phase contact angle between air bubble and solid immersed in water[71]

It is necessary to distinguish between situations where the air bubble is advancing or receding. The limiting static angles are referred to as advancing contact angle θ_A and receding contact angleθ_R respectively. In general $\theta_A > \theta_R$, which is very important in non-ideal surfaces[72].

Thermodynamically equilibrium of the three phase contact is expressed in terms of the respective interfacial tensions by the following expression known as Young's equation:

$$\gamma_{a/s} = \gamma_{s/l} + \gamma_{a/l} \cos\theta$$

Where $\gamma_{a/s}$, $\gamma_{s/l}$, and $\gamma_{a/l}$ are the interfacial tensions respectively of the solid/air, solid/liquid and liquid/air and θ is the contact angle. The change in the free energy of the displacement of a unit area of the solid/liquid interface is given by

$$\Delta G = \gamma_{a/s} - (\gamma_{s/l} + \gamma_{a/l})$$

This is a form of Dupre's equation. Combination of the Young and Dupre equations leads to the following expression for the free energy change[73]:

$$\Delta G = \gamma_{a/l} (\cos\theta - 1)$$

The free energy change for the attachment of the bubble has also been described in terms of the work of adhesion, which is defined as the work required to remove liquid from the surface of the solid leaving an adsorbed layer of water in equilibrium with saturated gas (air) phase.

Attachment of an air bubble to a mineral surface implies, thermodynamically, increase of the air /solid interface area and decrease of solid/water interface area. For attachment of the bubble $\cos\theta$ must be <1 for a finite contact angle. This is favored by

low $\gamma_{a/s.}$ Thus, low energy surfaces, that is solids with low surface energy are hydrophobic, those with high surface energies are hydrophilic. Most minerals have a high $\gamma_{a/s.}$ The objective of treatment with the collector is to create a surface with low $\gamma_{a/s}$ by adsorption[74].

Zisman and co-workers used the contact angle method to evaluate the $\gamma_{a/s}$ of low-energy solids. They plotted the surface energy tension of various liquids which wet the given solid partially, against the value of $\cos\theta$ of the angle measured with these liquids. The surface tension which $\cos\theta = 1$ denotes the so-called critical surface tension θ_C of the given solid. Only those solutions whose $\gamma_{a/l}$ is less than γ_c spread and wet the solid completely[75].

The concept of critical surface tension γ_c leads to a relationship between this quantity and flotation of minerals. If γ_c is equal to or greater than the surface tension of water, the mineral is hydrophilic. This is the natural property of most of the common minerals, which require a collector to make them hydrophobic. As the mineral surface is progressively made hydrophobic, its critical surface tension decreases[76].

In principle, one can also make a mineral floatable by controlling the surface tension of the liquid used as flotation medium. A mineral which is normally hydrophilic because its critical surface tension is greater than surface tension of water (72 mN/m) could in theory be made floatable in water if the surface tension of water is raised to a value higher than γ_c of the mineral. Dissolved electrolytes raise the surface tension of water, but the maximum value which can be attained does not exceed the γ_c of many common minerals. On the other hand, the minerals with lower critical surface tension than the surface tension of water could be made wettable in liquids with lower surface tension. The surface tension of water can be lowered by mixing ethanol. By progressively decreasing the surface tension (mixing controlled quantities of ethanol), the floatability and therefore the flotation recovery is progressively decreased until a liquid composition is reached in which the mineral exhibits no wettability. The surface tension of a liquid is now equal to the critical surface tension of the mineral[77, 78].

An important finding in experiments is that even the minerals recognized to be "inherently hydrophobic" contain hydrophilic sites and therefore, the floatability varies depending upon the fraction of such sites. This has been shown for several minerals. For example, molybdenite face has γ_a of 29 mN/m while molybdenite edge has a value > 72.5 mN/m, which makes it largely hydrophilic in water. Natural molybdenite prepared for flotation would have value between these two, in most cases closer to the value of the face[79].

1.10 Precipitated calcium carbonate nanoparticle

Calcium carbonate ($CaCO_3$) is used in large amounts in different industries such as plastics, rubbers, textile, pharmaceutical, biomaterials, paint and coating and pulp and paper industry. Precipitated calcium carbonate (PCC) is synthetic calcium carbonate ($CaCO_3$) with a higher purity than naturally occurring calcium carbonate (limestone). In the PCC process, calcium oxide (CaO, lime) is hydrated into calcium hydroxide (Ca (OH) $_2$, slaked lime), followed by carbonation of the hydroxide[80-82].

Calcium carbonate occurs abundantly in several natural minerals. It can be crystallized in a wide variety of morphologies, which makes it very versatile for a wide range of applications. The product of a controlled synthesis that produces a desired morphology and particle size is called precipitated calcium carbonate or PCC. PCC has a higher purity than natural or ground calcium carbonate (GCC) since impurities are removed in the production process. The most important crystalline forms of PCC are the rhombohedral calcite type, scalenohedral calcite type and orthorhombic acicular aragonite type. The scalenohedral form is favoured in most applications. There are several various types of PCC grades, but the purity of PCC is usually over 99% with density of 2700 kg/m^3. Important qualities of the limestone used for providing raw material for the PCC process are low manganese and iron content since these elements have a very negative influence on the brightness of the product. The iron content of PCC should be lower than approximately 0.1% for a commercial product[83-85].

It is foreseen that the world's PCC consumption in 2010 will be approximately 10^7 tons. One third of it is consumed by North American consumers and the rest mostly by Asian and Western European consumers. The largest consumers within these regions were companies in the USA, Japan, France, China and Finland[86].

Precipitated calcium carbonate can currently be produced by three different processes: a lime soda process, a calcium chloride process and a carbonation process. In the lime soda process, calcium hydroxide is reacted with sodium carbonate to produce a sodium hydroxide solution, from which the calcium carbonate is precipitated. This process is commonly used by alkali manufacturers, for whom sodium hydroxide recovery is the main objective, and the coarse PCC produced is only a by-product. In the calcium chloride process, calcium hydroxide is reacted with ammonium chloride, forming ammonia gas and a calcium chloride solution. After purification, this solution is reacted with sodium carbonate to form a calcium carbonate precipitate and a sodium chloride solution. This process is the simplest of the three but requires a low cost source of calcium chloride to be economical. Therefore, it is usually conducted in a satellite facility adjacent to a Solvay process soda ash plant. The third and most widely used process is the carbonation process because it can use cheap raw material. In this process, crushed limestone is burned in a lime kiln at about 1000 °C, where it decomposes into calcium oxide and carbon dioxide[87, 88].

$$CaCO_3(s) \longrightarrow CaO(s) + CO_2(g)$$

The dry CaO is slaked (hydrated) with water at temperatures of 30–50 °C, producing a $Ca(OH)_2$ slurry.

$$CaO(s) + H_2O(l) \longrightarrow Ca(OH)_2(s)$$

The slurry contains undissolved calcium hydroxide, calcium ions (Ca^{2+}) and hydroxide ions (OH^-). The calcium ion concentration in the slurry is dependent on the solvent solubility limit, which decreases as the temperature increases. Before carbonation, the process slurry is screened to remove impurities originating from the limestone. The slurry then reacts with CO_2 gas.

$$Ca(OH)_2(s) + CO_2(g) \longrightarrow CaCO_3(s) + H_2O(l)$$

The particle size, particle size distribution, particle shape and change of surface properties of the calcium carbonate particles can be controlled by controlling the reaction temperature, carbon dioxide partial pressure, flow rate of carbon dioxide, lime slurry concentration and agitator speed[89].

The carbonation temperature is in the range 41–90 °C for the scalenohedral form and -1 to 10 °C for the rhombohedral form. The threshold temperature for the aragonite structure is approximately 49 °C. CO_2 gas for the carbonation process dissolves into the water phase while it is bubbled through the slurry. During the reaction, the slurry is continuously under high shear agitation and the solid content is typically about 20%.

The pH of the lime slurry is 12 or higher at the beginning, but it decreases as the reaction proceeds, down to an equilibrium pH of 8 ± 1. The carbonation reaction is regulated by the solution equilibrium: as the calcium ions are converted to calcium carbonate and precipitated out, more calcium hydroxide dissolves to equalize the concentration of calcium ions. The rate of dissolution of $Ca(OH)_2$ into Ca^{2+} depends on the dissolution pressure and temperature, while the reaction rate of calcium ions combining with carbonate ions is immediate. Therefore, the rates of formation of calcium and carbonate ions are the first limitations for the reaction rate. With a pressurized reactor, the overall reaction rate is greater than with an atmospheric reactor and the solubility of carbon dioxide is higher at elevated pressure[90-92].

1.11 Silica nanoparticle

Colloidal silica is employed widely in industries as catalysts, polymers, optical and electronic materials. It is also used as a model system in catalysis, colloid science and materials science[93].

The first silica was produced on a commercial scale in 1850's and from waste glass. Since that time, a wide range of chemical and physical methods have been developed to produce a lot of silica products with different surface areas and porosity. Meanwhile, the Stober method has been studied over the last decade and its synthesis is well established to produce model silica dispersions. In the Stober method, spherical particles with a narrow size distribution are conveniently prepared by the hydrolysis and condensation of tetraethylorthosilicate (TEOS) using a mixture of water, alcohol (the cosolvent), and ammonia. Silica particles can be synthesized in the size range of 50 nm to 1000 nm. The resulting particles are electrostatically stabilized by negative surface charges arising from the dissociated silanol groups in the alkaline medium[94, 95].

Stober silica preparation method includes mechanisms of: particle nucleation and growth processes, particle microstructure and surface modification reactions using silane coupling agents and polymers. The preparation of Stober silica involves the ammonia catalyzed hydrolysis and condensation of TEOS in an aqueous alcohol (usually ethanol) solution and then the particles are electrostatically stabilized which comes from ionization of surface silanol groups in the ammonia mixture[96].

Aqueous silica sols have been shown to be colloidally stable at the isoelectric point (IEP) at pH 2-3 which has been explained due to repulsive hydration forces at the silica-water interface. In coagulation, on the other hand, counterion adsorbs onto the silica surface, a silanol group becomes blocked from hydrogen-bonding with water and this process dehydrates the hydroxylated silica surface[97, 98].

Colloidal stability of silica in a variety of solvents with different polarity and stability could originate from electrostatic, steric or electrosteric forces. An ideal colloid would be one with monodisperse, regular functional groups, and no or at least known porosity. Despite that there are very few systems that have all of these parameters; Stober silica nanoparticles possess many of the necessary properties[99].

Stober silica is one of the best studied colloidal systems which is employed as a model system in different areas. This process has several features such as below:

- The particles can be grown easily in the range of 20 nm to 1 micron
- Colloidally stable spherical particles with narrow particle size distribution for particles bigger than 50 nm
- These particles are non-porous
- They can be chemically modified

Particles prepared by the Stober method are electrostatically stabilized by the electrical double layer formed from the ionization of silanol groups which is done in aqueous NH_3 mixture[100].

In non-polar media, stabilization is achieved by employing polymers. Despite that many techniques have been used to prepare sterically stabilized dispersions, still there are

some problems such as swelling of the polymer lattices, irreproducibility, and controlling the nature of the polymer attached at the liquid/solid interface[101].

The modification of the surface of silica particles is done with reactive silanol groups utilizing the strength of the Si-O bond. Organosilanes ($RSi(OR')_3$) are grafted to the mineral making the inorganic surface more hydrophobic (Si-OSiR')[102].

For example, condensation reactions between colloidal silica and alkoxysilanes with different functional groups such as amino, mercapto, chloro or methacryl have been reported a lot. It is also possible to coat Stober silica with fluorescent dyes[103-106].

1.12 References:

1. Fuerstenau, D. W.; Raghavan, S., Flotation, AIME, New York, **1976**, p. 21.
2. Schramm, L.; Morrison, S.; Stasiuk, E., Fuel processing technology **1998**, 56, (3), 243- 261.
3. Pouet, M. F.; Grasmick, A., Water science and technology **1995**, 31, (3-4), 275-283.
4. Hornfeck, K., CONSERV. RECYCLING. **1987**, 10, (2-3), 125-132.
5. Harvey Alter, Resources, Conservation and Recycling **2005**, 43, (2), 119- 132.
6. Adamson, A. W.; Gast, A. P., Physical chemistry of surfaces, Sixth edition, John Wiley & Sons, Inc.
7. Zouboulis, A. I.; Matis, K. A.; Lazaridis, N. K.; Golyshin, P. N., Minerals Engineering **2003**, 16, (11), 1231- 1236.
8. Roa, S. R.; Leja, J., Surface chemistry of froth flotation, Volume 1, Plenum publisher, New York, **1982**.
9. Masliyah, J.; Zhou, Z. J.; Xu, Z.; Czarnecki, J; Hamza, H., Canadian Journal of chemical engineering **2004**, 82, (4), 628- 654.
10. Hardie, C. A.; Leichtle, G. F.; Watson, J. A.; Finch, J. A.; Gomez, C. O., Application of mineral processing techniques to the recycling of wastepaper, CIM bulletin **1999**, 92, (1031), 131- 137.
11. Singh, R. P.; Nayak, B. R.; Biswal, D. P.; Tripathy, T.; Banik, K., Mat. Res. Innovat. **2003**, 7, 331-340.
12. Adkins, S. J.; Pears, M. J., Minerals Engineering, **1992**, 5, 295- 310.
13. Wiese, J.; Harris, P.; Bradshaw, D., Mineral Engineering **2006**, 19, 1290- 1300.
14. Finch, J. A., Flotation: Chemical aspects, Introduction to mineral processing Course notes, McGill University, **2009**.
15. Deng, T.; Yu, S.; Lotter, N. O.; Di Feo, A., 42nd annual meeting of the Canadian mineral processors, **2010**.
16. Mainza, A. N.; Simukanga, S.; Witika, L. K., Mineral Engineering **1999**, 12, (5), 571- 577.
17. Somasundaran, P.; Moudgil, B. M., Reagents in mineral technology, Marcel Dekker Inc., New York, **1988**.
18. Roa, S. R.; Leja, J., Surface chemistry of froth flotation, Volume 2, Plenum publisher, New York, **1982**.
19. Gaudin, A. M., Flotation, McGraw-Hill Inc., **1957**.
20. Massola, C.P.; Chaves, A.P.; Lima, J.R.B.; Andrade, C.F., Minerals Engineering **2009**, 22, 315–318.
21. Ma, X.; Bruckard, W. J.; Holmes, R., Int. J. Miner. Process. **2009**, 93, 54–58.
22. Hodgson, M.; Agar, G. E., Canadian Metallurgical Q. **1989,** 28, (3), 189-198.
23. Grano, S. R.; Prestidge, C. A.; Ralston, J., International Journal of Mineral Processing **1997**, 52, 161-186.
24. Vucinic, D. R.; Lazic, P. M.; Rosic, A. A., Colloids and Surfaces A: Physicochem. Eng. Aspects **2006**, 279, 96–104.

25. Fuerstenau, D.W.; Pradip, T., Advances in Colloid and Interface Science **2005**, 114, 9 – 26.
26. Pelton, R. H., The electrical double layer, Interfacial Engineering Course note, McMaster University, **2009**.
27. Fuerstenau, D.W.; Shibata, J, Int. J. of mineral processing **1999**, 56, (3), 205- 217.
28. Adkins, S. J.; Pearse, M. J., Minerals Engineering **1992**, 5, (3-5), 295- 310.
29. Hu, Y.; Liu, X.; Xu, Z., Minerals Engineering **2003**, 16, 219- 227.
30. Pietrobon, M. C.; Grano S. R.; Sobieraj, S.; Ralston, J., Minerals Engineering **1997**, 10, (8), 775- 786.
31. Nagaraj, D. R.; Rothenberg, A. S.; Lipp, D. W.; Panzer, H. P., International Journal of Mineral Processing **1987**, 20, 291- 308.
32. Liu, Q.; Wannas, D.; Peng, Y., International Journal of Mineral Processing **2006**, 80, 244- 254.
33. Chandra, A. P.; Gerson, A. R., Advance in colloid and interface sciences **2009**, 145, 97- 110.
34. Zhou, Z. A.; Xu, Z.; Finch, J. A., Minerals Engineering **1994**, 7, (9), 1073- 1084.
35. Navidi Kashani, A. H.; Rashchi F., Minerals Engineering **2008**, 21, 967- 972.
36. Gregory, J., Critical reviews in Environmental Control **1989**, 19, (3), 185- 230.
37. Song, S.; Lopez, A.; Reyes, J. L.; Lara, C., Minerals Engineering **2000**, 14, (1), 87- 98.
38. Giesekke, E.W., Int. J. of mineral processing **1983**, 11, (1), 19- 56.
39. Buckley, A. N.; Woods, R., Applied surface science **1987**, 27, (4), 437-452.
40. Trahar, W. J., Int. J. of mineral processing **1981**, 8, (4), 289- 3327.
41. Subrahmanyam, T. V.; Forssberg, K. S., International Journal of Mineral Processing **1988**, 23, 33- 53.
42. Subrahmanyam, T. V.; Forssberg, K. S., Minerals Engineering **1988**, 1, (1), 41- 52.
43. Trahar, W. J.; Warren, L. J., International Journal of Mineral Processing **1976**, 3, 103- 131.
44. Dai, Z.; Fornasiero, D.; Ralston, J., Advances in colloid and interface science **2000**, 85, (2- 3), 231- 256.
45. Dai, Z.; Fornasiero, D.; Ralston, J., Journal of colloid and interface science **1999**, 217, (1), 70- 76.
46. Zhou, Z. A.; Xu, Z.; Finch, J. A.; Masliyah, J. H.; Chow, R. S., Minerals Engineering, **2009**, 22, 419- 433.
47. Eastham, R. D.; Duncan, R., A guide to water, electrolyte, and acid-base metabolism, Wright-PSG publication, **1983**.
48. Erickson, G. A., Anal. Chim. Acta **1979**, 12, 375- 383.
49. Sui, C. C.; Lee, D.; Casuge, A.; Finch, J. A., Mineral and Metall. Process, **1999**, 16, 55- 62.
50. Bockris, J. O'M.; Rand, D. A. J.; Welch, B. J., Trends in electrochemistry, Plenum Press, **1977**.
51. Chander, S.; Briceno, A.; Pang, J., Minerals Metallurg. Process, **1992**, 9, 7-12.

52. Collins, G. L.; Jameson, G. J., Chemical Engineering Science **1977**, 32, (3), 239-246.
53. Elimelech, M.; Williams, R. A.; Jia, X.; Gregory, J., Particle deposition and aggregation: Measurement, Modeling and Simulation, Butterworth- Heinemann, **1995**.
54. Somasundaran, P., J. of Coll. & Inter. Sci. **1968**, 27, (4), 659-666.
55. Dibbs, H. P., Determination of the zeta potential of minerals, Canada mines branch publication, **1972**.
56. Mani, H.; Xu, M.; Quinn, P., The effect of ultramafic mineralogy on pentlandite flotation, Fundamentals of Mineral Processing and the Environment, Sudbury, Ontario, **1997**, 63-76.
57. Fielden, M. L.; Hayes, R. A.; Ralston, J., Langmuir **1996**, 12, (15), 3721- 3727.
58. Mishchuk, N.; Ralston, J.; Fornasiero, D., Journal of physical chemistry A **2002**, 106, (4), 689- 696.
59. Hunter, R.J., Colloid Science: Zeta Potential in Colloid Science: Principles and Applications, Academic Press, London, **1981**.
60. Pushkarova, R.A.; Horn, R.G., Colloids and Surfaces A: Physicochemical and Engineering Aspects **2005**, 261, (1-3), 147-152.
61. Nguyen, A.V.; Schulze, H.J., Colloidal Science of Flotation, Marcel Dekker, **2004**.
62. Snoswell, D.R.E.; Duan, J.; Fornasiero, D.; Ralston, J., Journal of Physical Chemistry B **2003**, 107, (13), 2986-2994.
63. Ishida, N.; Higashitani, K., Publications of the Australasian Institute of Mining and Metallurgy(Centenary of Flotation Symposium), **2005**, 481-486.
64. Yoon, R.H.; Mao, L., Journal of Colloid and Interface Science **1996**, 181, (2), 613- 626.
65. Miettinen, T.; Ralston, J.; Fornasiero, D., Minerals Engineering **2010**, 23, 420-437.
66. Adamson, A. W., Physical Chemistry of surfaces, John Wiley, New York, **1997**.
67. Finch, J; Smith, G. W., Mineral Sci. Eng. **1979**, 11, 36- 63.
68. Fowkes, F. M., Contact angle, Wettability, and adhesion, American Chemical Society, Washington D C, **1963**.
69. Hayes, R. M.; Price, D. M.; Ralston, J.; Smith R. W., Minerals Process. Extract. Metall., **1987**, 2, 1- 20.
70. Dourado, F.; Gama,F. M.; Chibowski, E.; Mota, M., J. Adhesive Sci. Tech. **1998**, 12 (10), 1081- 1090.
71. Nguyen, A. V.; Ralston, J.; Schulze, H. J., Int. J. Miner. Process. **1998**, 53, 225-249.
72. Good, R. J.; Koo, M. N., Journal of Colloid and Interface Science **1979**, 71, (2), 283-293.
73. Van Oss, C. J., Colloids and surfaces B: Biointerfaces **1995**, 5, 91- 110.
74. Evans, R. F., Industrial & Engineering Chemistry **1954**, *46* (11), 2420-2424.
75. Shafrin, E. G.; Zisman, W. A., J. of Phys. Chem. **1967**, 71(5), 1309-1316.
76. Ozcan, O., International Journal of Mineral Processing **1992**, 34, 191-204.

77. Hornsby, D. T.; Leja, J., Colloids & Surfaces **1983**, 7, 339.
78. Hornsby, D. T.; Leja, J., Colloids & Surfaces **1980**, 1, 425.
79. Kelebek, S.; Yoruk, S.; Smith, G. W., Sep. Sci. Tech. **2001**, 36, 145-157.
80. Li, L.; Collis, A.; Pelton, R., J. Pulp Paap. Sci. **2002**, 28, 267-273.
81. Zhang, H.; Chen, J. F.; Zhou, H. K.; Wang, G. O.; Yun, J., J. Mater. Sci. Lett. **2002**, 21, (16), 1305-1306.
82. Kreklau, B.; Sittinger, M.; Mensing, M. B.; Voigt C.; Berger, G.; Burmester, G. R.; Rahmanzadeh, R.; Gross, U., Biomater. **1999**, 20, (18) 1743-1749.
83. Kemperl, J.; Macek, J., Int. J. Miner. Process. **2009**, 93, 84-88.
84. Kawano, J.; Shimobayashi, N.; Kitamura, M.; Shinoda, K.; Aikawa, N., J. Crystal Growth **2002**, 237-239, 419-423.
85. Park, A.; Fan, L. S., Chem. Eng. Science **2004**, 59, 2541-2547.
86. The economics of precipitated calcium carbonate, 6th ed., Roskill Informatics Service, London, UK.
87. Tier, S.; Eloneva, S.; Zevenhoven, R., Energy Conv. Manag. **2005**, 46, 2954-2979.
88. Lopez-Periago, A. M.; Pacciani, R.; Carcia-Gonzalez, C.; Vega, L. F.; Domingo, C., J. supercritical fluids **2010**, 52, (3), 298-305.
89. Kitamura, M., J. Crystal Growth **2002**, 237-239, 2205-2214.
90. Kim, W. S.; Hirasawa, I.; Kim, W. S., Ind. Eng. Chem. **2004**, 43, 2650-2657.
91. Colfen, H., Curr. Op. Coll. Interface Sci. **2003**, 8, 23-31.
92. Uebo, K.; Yamazaki, R.; Yoshida, K., Adv. Powder Tech. **1992**, 3, (1), 71-76.
93. Badley, R. D.; Ford, W. T., Org. Chem. **1989**, 54, 5437.
94. Stober, W.; Fink, A., J. Coll. Inter. Sci. **1968**, 26, 62-69.
95. Badley, R. D.; Ford, W. T.; McEnroe, F. J.; Assink, R. A., Langmuir **1990**, 6, 792-801.
96. De Haan, J. W.; Van Den Bogaert, H. M.; Ponjee, J. J. ; Van De Ven, L. J. M., J. Coll. Inter. Sci. **1986**, 110, (2), 591-600.
97. Sasaki, S.; Maeda, H., J. Colloid Int. Sci. **1994**, 167, 146.
98. Frolov, Y. G.; Shabanova, N. A., Langmiur **1987**, 3, 640.
99. Ketelson, H. A.; Brook, M. A.; Pelton, R. H., Chem. Mater. **1995**, 7, 1376-1383.
100. Bogush, G. H.; Tracy M. A.; Zukoski IV, C. F., Non-Cryst. Solids **1988**, 104, 95.
101. Zhao, W.; Pacard, E.; Chaix-Bauvais, C.; Pichot, C.; Brook, M. A., Coll. & Surf. A: Phys. Eng. Asp. **2009**, 339, 26-34.
102. Jesionowski, T., Composite Interfaces **2009**, 16, 115-129.
103. Pham, K. N.; Fullston, D.; Sagoe-Crentsil, K., Aus. J. Chem. **2007**, 60, 662-666.
104. Chen, S.; Hayakawa, S.; Shirosaki, Y.; Fujii, E.; Kawabata, K.; Tsuru, K.; Osaka, A., J. Am. Ceram. Soc. **2009**, 92, (9), 2074-2082.
105. Liu, X.; Xing, J.; Guan, Y.; Shan, G.; Liu, H., Colloids and Surfaces **2004**, 238, 127-131.
106. Rahman, I. A.; Jafarzadeh, M.; Sipaut, C. S., Ceramics International **2009**, 35, 1883-1888.

Chapter 2

Preparation and characterization of uniform nickel sulfide thin films on glass for model adhesion studies

2.1 ABSTRACT

The first step in this project was preparing a very uniform thin layer of nickel sulfide for model adhesion studies. The method employed was successive ionic layer adsorption and reaction (SILAR), which was based on adsorption of a cationic precursor and reacting it with an anionic precursor. The profilometry, AFM and SEM results show a weak deposited layer of nickel sulfide on glass, which was very uneven at low SILAR deposition cycles and very porous at high SILAR deposition cycles.

Another method which is possible to employ is "self assembled monolayer (SAM)" which is based on the reaction of a hydrolyzed mercaptosilane with a glass substrate to have mercapto functional group on top and consequent reaction of the mercapto functional group with nickel and iron chlorides to have uniform monolayer of nickel/iron sulfide on top of the glass surface.

2.2 INTRODUCTION

Preparing nano-sized, smooth mono-layers with straightforward synthetic procedures is a very important goal in surface sciences. Uniform, conformal thin films have a wide range of applications in modern technology including semiconductor microelectronics, displays, optical filters, magnetic information storage and catalysis[1]. Also, development of novel methods for producing materials at the nanometer scale is extremely interesting[2, 3].

In this way, there are different approaches to prepare nanoscale thin films such as self-assembled monolayer, gas phase synthesis, solid state preparation, vapor deposition, atomic layer deposition, and electroplating[4-6].

Furthermore, there has been a significant increase in interest to synthesize inorganic materials under mild conditions such as metal sulfide materials with controlled architecture for specific applications in the electronics industry or photovoltaic applications in the last decade [7]. Among the family of metal sulfides, nickel sulfides have attracted much attraction because of their potential as a transformation toughening agent for materials used in semiconductor applications and their applications as catalysts or as

coatings for photogalvanic cells[8, 9]. However, nickel sulfide is powder and applying it on a substrate is very challenging[10].

Nickel sulfide thin films can be employed as solar selective coatings, IR detectors and as storage electrode in photoelectrochemical storage devices[11]. Also, Nickel sulfides can exist in a wide variety of phases. They can occur as NiS_2 (pyrite), Ni_3S_4 (spinel), nickel deficient form ($Ni_{1-x}S$), and many metallic phases of compositions between NiS and Ni_3S_2[12].

Unfortunately, publications about deposition of nickel sulfides thin films are very scarce. There are some reports about the application of nickel sulfide thin films on glass substrate using different precursors such as nickel sulfate and thioacetainide solutions in alkaline medium or preparing polycrystalline nickel sulfide thin films in acidic medium with nickel sulfate and sodium thiosulophate[13, 14].

The procedure we employed for application of nickel sulfide thin films was successive ionic layer adsorption and reaction (SILAR) method which is a relatively simple and less expensive method[15]. This method is suitable for large area deposition of metal sulfide thin films. In any single SILAR deposition cycle, the substrate is immersed into cationic and anionic precursor solutions (adsorption and reaction) and rinsed with distilled water in between to avoid homogeneous precipitation. The time durations for adsorption, reaction and rinsing are important. In the SILAR deposition method, thickness of the layer is determined by the number of deposition cycles[16].

2.3 EXPERIMENTAL

2.3.1 Materials: Nickel sulfate and sodium sulfide were purchased from Sigma Aldrich. Polyvinylamine (PVAm) (Polymin PR 8178) was purchased from BASF. Liquid ammonia was lab grade and distilled water conductivity was 18μS/cm.

2.3.2 SILAR deposition[15]

0.1 M nickel sulfate and 0.5 M sodium sulfide solutions were employed as cationic and anionic precursors respectively. The pH of nickel sulfate solution was adjusted to 8 by adding liquid ammonia. The pH of sodium sulfide solution was pH 12.

Each solution was taken into 50 ml beakers separately. Samples were rinsed with distilled water between each immersion and all the experiments were carried out at ambient temperature. Figure 2.1 shows SILAR deposition method schematically.

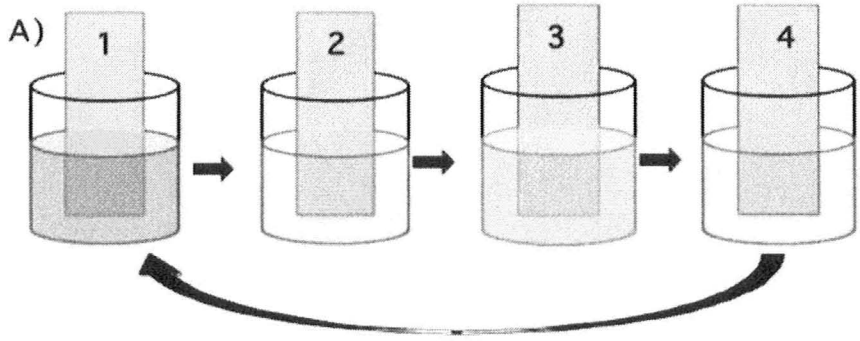

Figure2.1 Schematic procedure of SILAR deposition method, solution 1: nickel sulfide, 2: distilled water, 3: sodium sulfide, 4: distilled water

Every time the substrate was immersed in the nickel sulfide solution, nickel ions adsorbed on the surface of the glass. The duration for immersion was 60 seconds. Consequently, sulfide ions react with adsorbed nickel ions when the glass substrate is immersed in sodium sulfide for another 60 seconds. In this way, a very thin layer of nickel sulfide was formed on the glass surface. By rinsing the surface for 40 seconds between each immersion, un-adsorbed and un-reacted ions or powdery nickel sulfide materials were washed out from the surface. This is one SILAR deposition cycle. To prepare a very uniform, smooth, thin layer of nickel sulfide on glass, this cycle was repeated for 10, 20, 40 and 60 times.

2.3.3 Profilometry

To characterize the roughness of nickel sulfide thin film, profilometry (Wyko NT 1100, Veeco metrology group) was carried out. For PSI measuring mode, magnification was adjusted to 20.64, sampling was from 406.98 nm and array size was 736X480. For VSI measuring mode, magnification was adjusted to 5.12, sampling was from 1.64 μm and array size was 736X480.

2.3.4 Atomic Force Microscope (AFM)

AFM technique was employed to study the roughness of nickel sulfide thin film. The AFM tip is first brought (manually) close to the sample surface, and then the scanner makes a final adjustment in tip–sample distance. The tip then scanned across the sample by moving the tip relative to the sample. A laser beam aimed at the back of the cantilever–tip assembly reflects off the cantilever surface to a split photodiode, which detects the small cantilever deflections and a feedback loop maintains constant tip–sample separation by moving the scanner in the z direction to maintain the setpoint deflection. Finally, the distance the scanner moves in the z direction is stored in the computer relative to spatial variation in the *x-y* plane to generate the topographic image of the sample surface.

2.3.5 Scanning Electron Microscopy (SEM)

SEM was carried out to study the deposition of nickel sulfide thin film to the glass substrate. The magnification used was 25,000 for all samples.

2.4 RESULTS AND DISCUSSION

The results of profilometry for samples with 10, 20, 40 and 60 SILAR deposition cycles are shown in Figures 2.2 to 2.5 respectively.

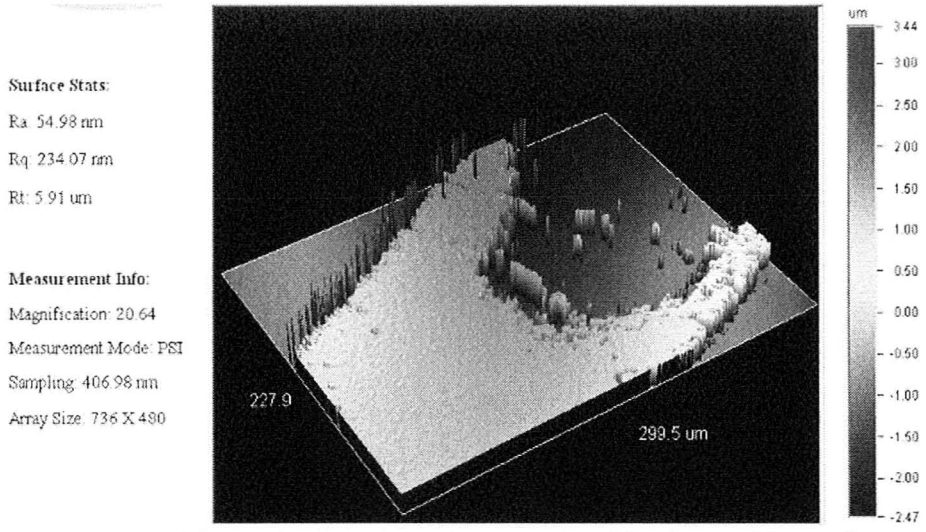

Figure2.2 profilometry image for 10 SILAR deposition cycles

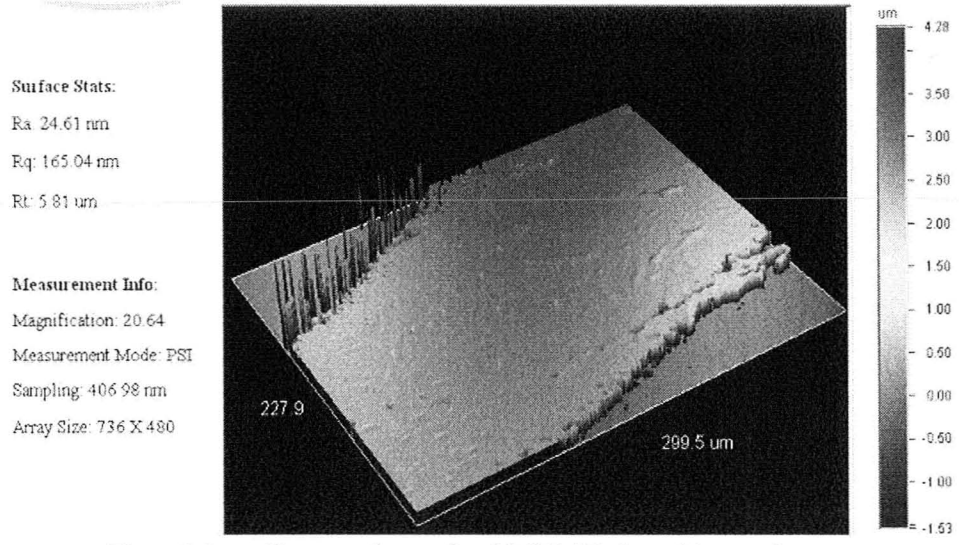

Figure2.3 profilometry image for 20 SILAR deposition cycles

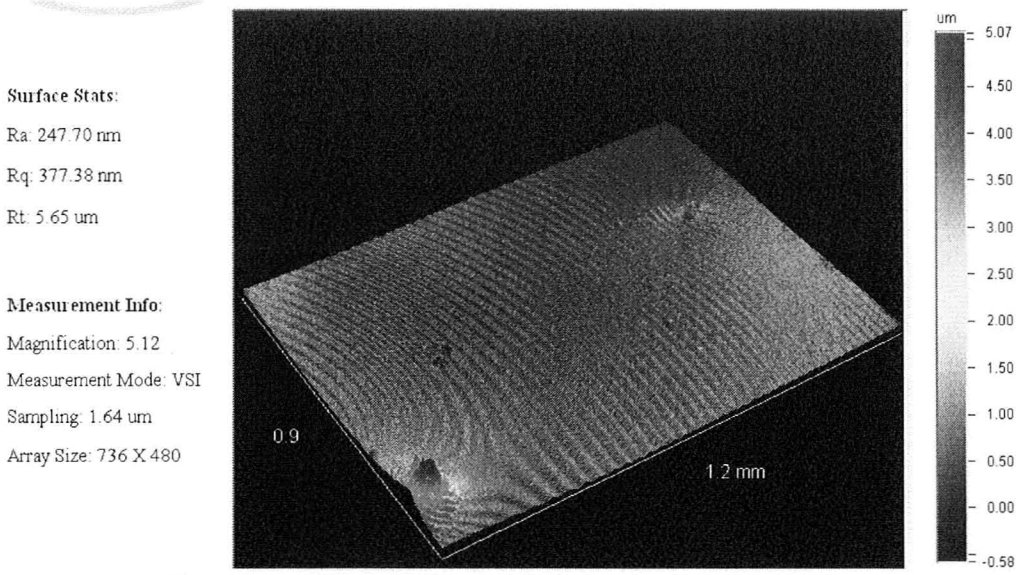

Figure2.4 profilometry image for 40 SILAR deposition cycles

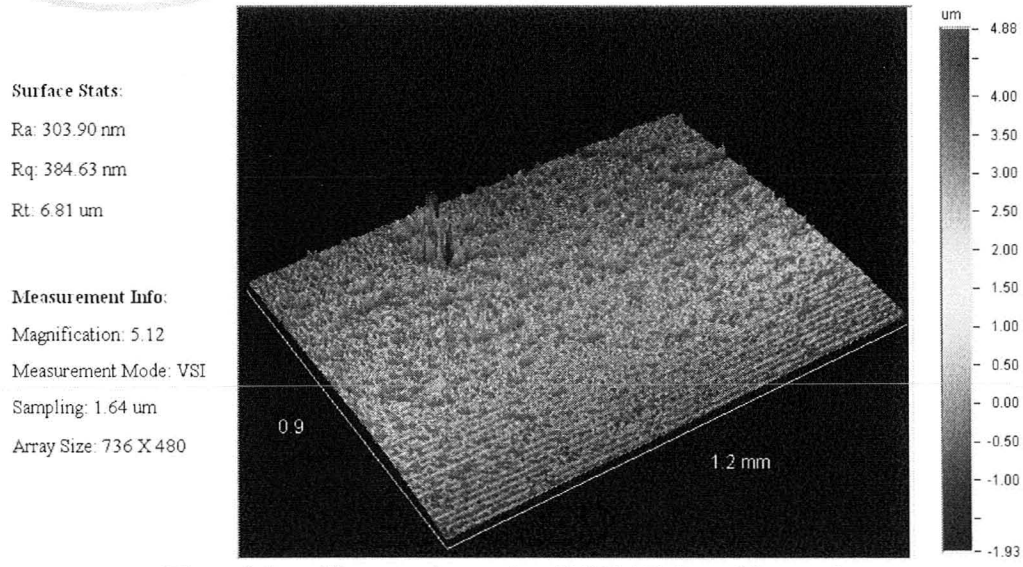

Figure2.5 profilometry image for 60 SILAR deposition cycles

The profilometry images show that in 10 and 20 SILAR deposition cycles; there are lots of uncoated spots which is not desirable and also by increasing the deposition cycles to 40 and 60 cycles, roughness of film increased dramatically. Moreover, adhesion of nickel sulfide thin films to glass substrate is not adequate to hold the film on the substrate. In fact, they easily rub off with flowing water.

Therefore, PVAm was applied as a primer with dipping the substrate in the solution in order to enhance the adhesion. The results showed that applying PVAm primer not only does not enhance the adhesion, but also; increased the roughness of the nickel

sulfide thin film. Figure 2.6 shows the profilometry image of 20 SILAR deposition cycles film with PVAm as a primer.

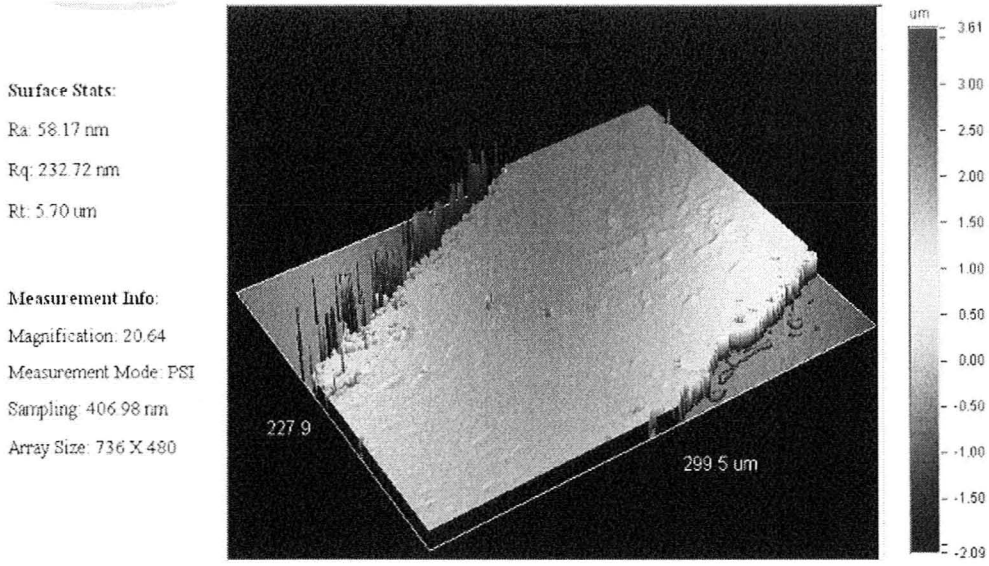

Figure2.6 profilometry image for 20 SILAR deposition cycles with PVAm as a primer

In the next step, the films prepared with 20 and 40 SILAR deposition cycles were selected for more characterization with AFM and SEM tests. But, the sample with 40 SILAR deposition cycles was very rough for AFM, then; AFM was just carried out for samples with 20 SILAR deposition cycles and also glass surface for comparison. Figures 2.7 and 2.8 show the results of AFM for bare glass substrate and nickel sulfide surface prepared with 20 SILAR deposition cycles.

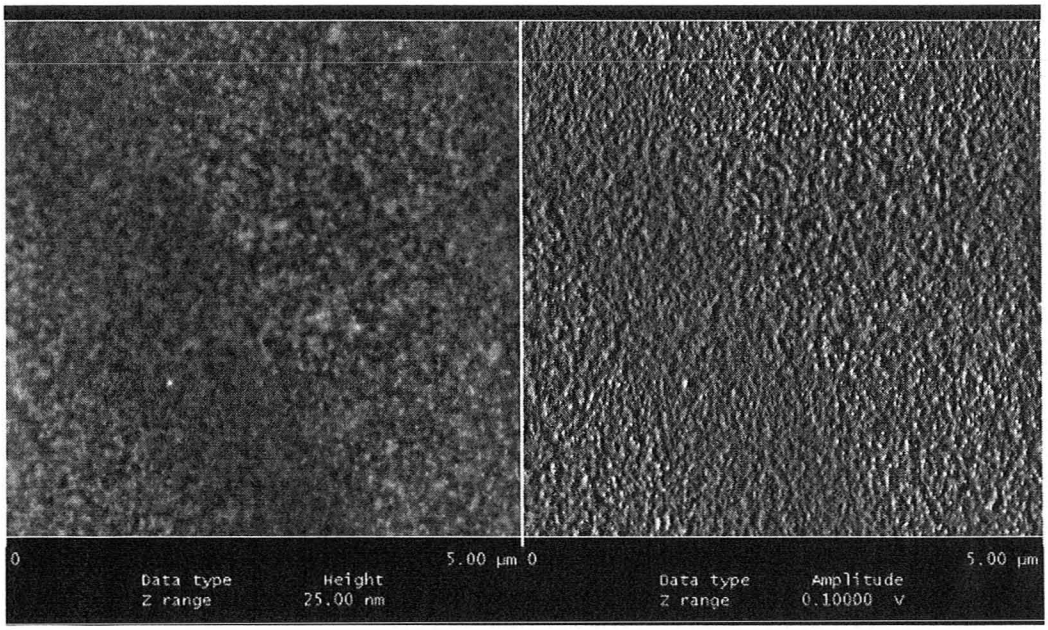

Figure2.7 AFM image for glass substrate

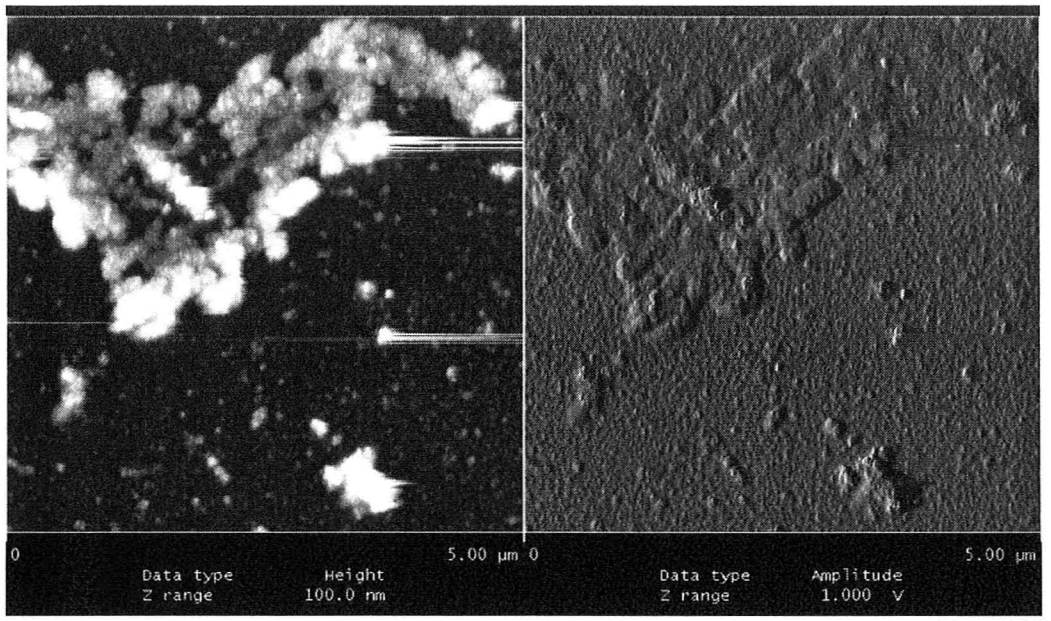

Figure2.8 AFM image for nickel sulfide sample prepared with 20 SILAR deposition cycles

AFM results show that preparing a very uniform nickel sulfide thin film that can coat all the substrate is not possible by applying SILAR deposition for 20 cycles. On the other hand, the thicker samples prepared by increasing SILAR deposition cycles are not appropriate to be studied with AFM.

Also, SEM was carried out to further study the deposition of nickel sulfide to glass substrate. SEM images of nickel sulfide thin films prepared with 20 and 40 SILAR deposition cycles are shown in Figures 2.9 and 2.10 respectively.

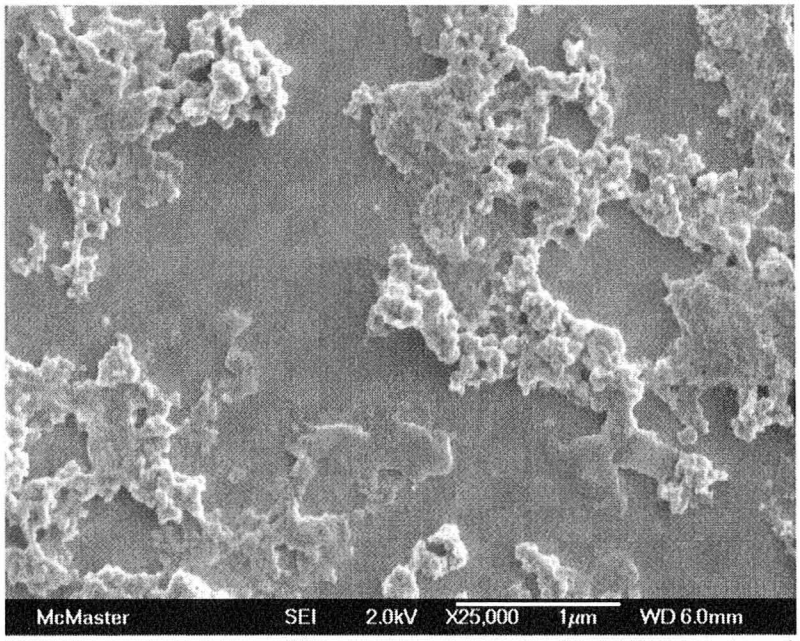

Figure2.9 SEM image for nickel sulfide sample prepared with 20 SILAR deposition cycles

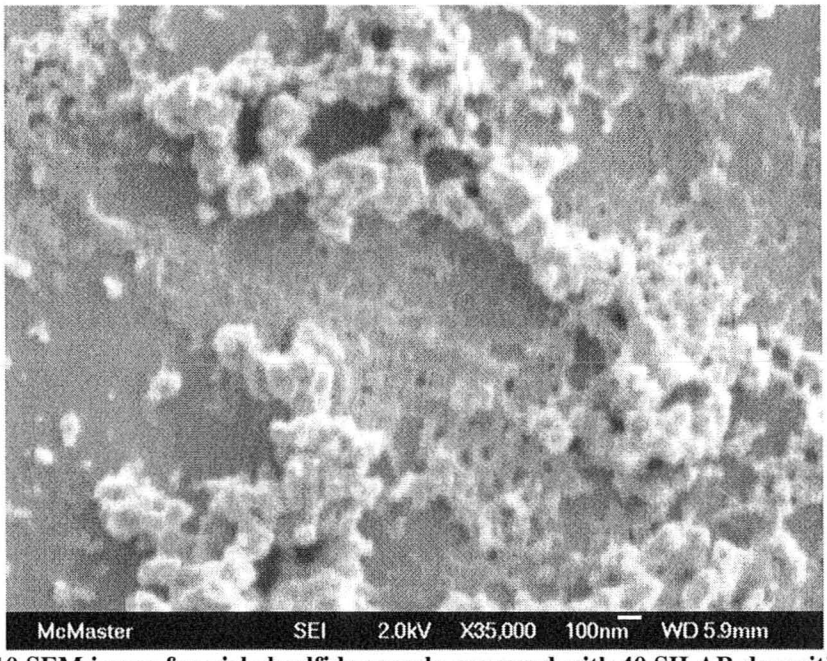

Figure2.10 SEM image for nickel sulfide sample prepared with 40 SILAR deposition cycles

SEM results also confirm that preparing nickel sulfide thin film by SILAR deposition method results in some aggregation of nickel sulfide on the glass substrate.

2.5 Suggestion for future work

Adsorbing self assembled monolayers (SAMs) is a very good method to form high density and smooth surfaces. SAM with special chemical groups can react with complementary groups to have a new covalent bond with the growth of the monolayer[17-19]. Therefore, it is possible to apply similarly dense grown monolayers with chosen functional groups on top of the surface[20]. If the substrate is glass, the reaction of trialkoxysilanes in solution is a straightforward technique as depicted in Figure 2.11[21].

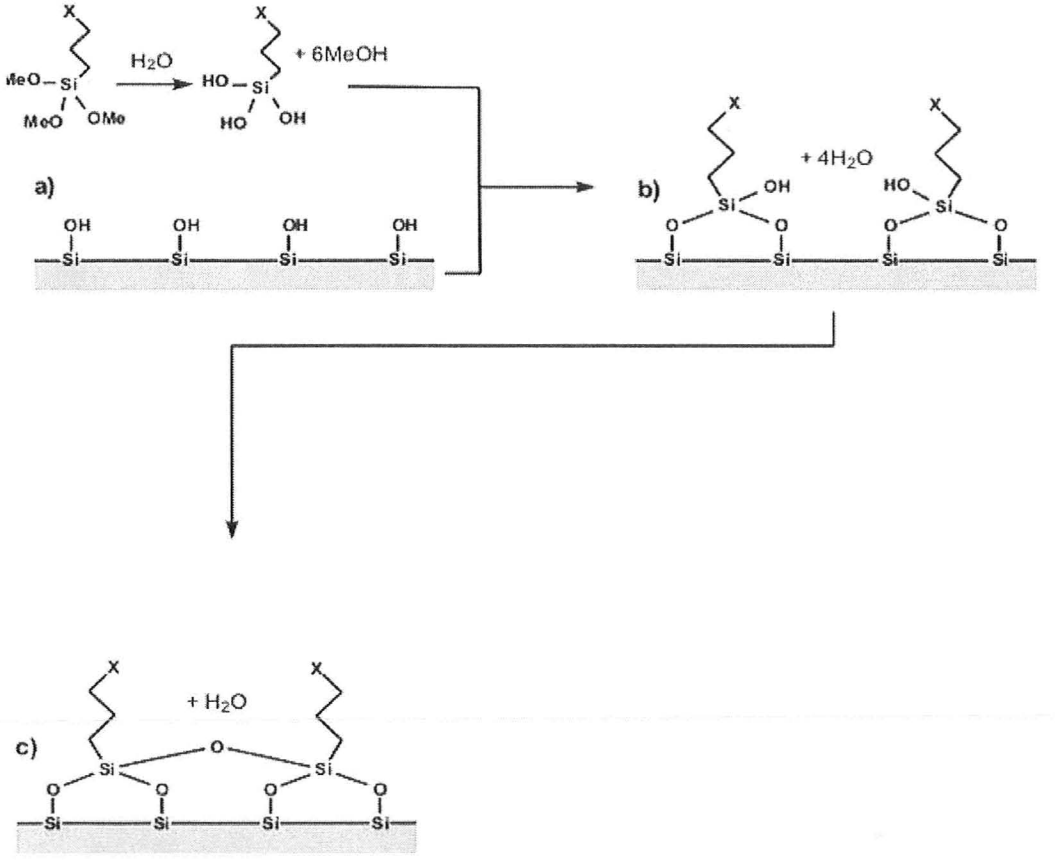

Figure2.11 The schematic reaction of trialkoxysilane with glass[21]

In this procedure, the surface silanol groups react with the Si-OH groups of the hydrolyzed trialkoxysilane (stage a), with the formation of $Si_{(surface)}$-O-Si bridges (stage b). The remaining Si-OH groups of the hydrolyzed trialkoxysilanes are positioned in such a way that Si-O-Si bridges can be formed with similar neighbors (stage c).

Therefore, it is possible to have a straightforward method to obtain a high density SAM of mercaptopropyltrimethoxysilane (MPTS) on glass to have a layer of terminal – SH groups.

In the next step, it is possible to graft nickel and iron on MPTS covered glass slides by means of the nickel chloride and iron chloride as shown in Figure 2.12.

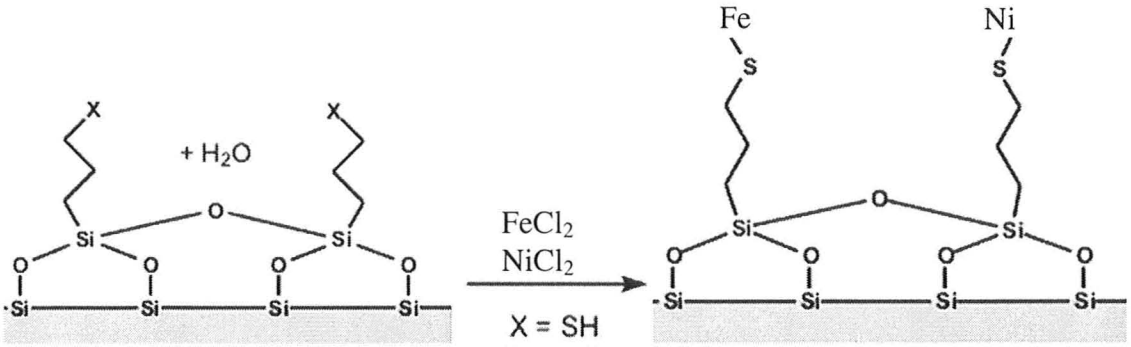

Figure2.12 Schematic reaction of -SH terminated SAM with nickel and iron chloride

2.6 Conclusions

This work was one of the challenges for us and the main conclusions are as below:

We have a very uneven non-uniform film in lower SILAR deposition cycles which cannot cover all the substrate and a very porous coating in higher SILAR deposition cycles. Also, adhesion of this film to the glass substrate is very weak and it was rubbed off easily by washing with distilled water.

Indeed, Sartale et al.[15] determined the thickness of nickel sulfide film by gravimetric weight difference method using sensitive micro balance, assuming film density as bulk density of nickel sulfide and did not study the surface characteristics of films such as roughness and uniformity that is very critical for model adhesion studies.

Self-assembled monolayer (SAM) method is a very good method to form uniformed and smooth surfaces. By hydrolyzing mercaptopropyltrimethoxysilane (MPTS) and applying on the glass surface, it is possible to have a layer with terminal –SH groups. Simulating nickel iron sulfide is also possible by reacting mercapto groups with nickel and iron chlorides.

2.7 References:

1. Lim, B. S.; Rahtu, A.; Gordon, R. G., Nature materials **2003**, 2, 749.
2. Lakshmi, B.; Patrissi, C. J.; Martin, C. R., Chem. Master. **1997**, 9, 2544.
3. Schmidt, G., Chem. Rev. **1992**, 92, 1709.
4. Hemakanthi, G.; Dhathathreyan, A.; Ramasami, T.; Mobius, D., Thin solid films **2001**, 384, 206-211.
5. Yang, T. S.; Cho W.; Kim, M.; An, K.; Chung, T.; Kim, C. G.; Kim, Y., J. Vac. Sci. Technol. A. **2005**, 23, (4), 1238.
6. Chae, J.; Park, H. S.; Kang, S. W., Electrochemical and solid-state letters **2002**, 5, (6), C64.
7. O'Brien, P.; Park, J. H.; Waters, J., Thin solid films **2003**, 431-432, 502-505.
8. Yu, S. H., Yoshimura, M., Advanced functional materials **2002**, 12, 277-285.
9. Kriven, W. M., Material science engineering A **1990**, 127, 249.
10. Zhang, L.; Yu, J. C.; Mo, M.; Wu, L.; Li, Q.; Kwong, K. W., J. Am. Chem. Soc. **2004**, 126, 8116-8117.
11. Johnson, T. H., Proc. Int. Opt. Eng. **1984**, 433, 60-94.
12. O'Brien, P.; Waters, J., Chem. Vap. Deposition **2006**, 12, 620-626.
13. Pramanik, P.; Biswas, S., J. Solid State Chem. **1986**, 65, 145-147.
14. Uplane, M. D.; Patil P.S.; Lokhande, C.D., Bull. Electrochem. **1995**, 11, 569.
15. Sartale, S.D.; Lokhande, C.D., Materials Chemistry and Physics **2001**, 72, 101-104.
16. Nicolau, Y. F.; Dupuy, M.; Brunel, M., J. Electrochem. Soc. **1990**, 137, 2915.
17. Ruckenstein, E.; Li, Z. F., Adv. Colloid Interface Sci. **2005**, 113, 43-63.
18. Love, J. C.; Estroff, L. A.; Kriebel, J. K.; Nuzzo, R. G.; Whitesides G. M., Chem. Rev. **2005**, 105, 1103-1169.
19. Lummerstorfe, T.; Hoffmann, H., J. Chim. Phys. B **2004**, 108, 3963-3966.
20. Seo, K.; Konchenko, A. V.; Lee, J.; Bang, G. S.; Lee, J., J. Am. Chem. Soc. **2008**, 130, 2553-2559.
21. Pallavicini, P.; Dacarro, G.; Galli M.; Patrini, M., J. Coll. Inter. Sci. **2009**, 332, 432-438.

Chapter 3

First generation inorganic particles as flotation collectors

3.1 ABSTRACT

Commercial grades of precipitated calcium carbonate (PCC) and colloidal silica were prepared and employed as collectors for flotation of glass beads. Also, stearic acid treatments were carried out on untreated PCC samples. Despite that the mean particle size of PCC particles are in the nano-range, they aggregate in aqueous solution and particle size increased to the micron range.

Therefore, deposition of these particles to glass beads was very low and consequently flotation results were not satisfactory. SEM images confirmed low deposition of PCC particles to glass beads. A wide range of methods have been tried to decrease the particle size of PCC particles but none of them were successful.

In another series of experiments, colloidal silica was employed as a collector for flotation of glass beads. These particles have colloidal stability at low pH values but they aggregated when the pH was increased to 9 which is the flotation operating pH. The inorganic particles did not show good deposition to glass beads or good flotation ability from pH 4 to 9. The reasons could be hydrophilicity of colloidal silica at low pH and their aggregation at high pH.

3.2 INTRODUCTION

3.2.1 Precipitated Calcium Carbonate (PCC)

Ground natural calcite is one of the oldest manufactured powders and precipitated calcium carbonate (PCC) was first prepared almost a hundred years ago. Well-defined PCC particles with a narrow size distribution, uniform shape and definite crystal structure have many applications in industry. The mentioned characteristics also play a crucial role in PCC properties and their control is closely related with the method of their production and the process parameters[1]. Also, much attention has been paid to the fabrication of hydrophobic and super-hydrophobic PCC particles since calcite is the most abundant mineral on earth and finds wide range of applications in industries such as plastics, textiles, rubbers, paints, pigments, paper and pharmaceuticals[2].

The synthesis of nano-PCC is being given more and more attention because of its excellent properties and increasing market demand [3]. The surface of PCC is often rendered hydrophobic by a variety of surface modifiers such as fatty acids, phosphates, silanes, titanates, or zirconates [4].

Therefore, improving wetting and dispersion as well as uniform size distribution of particles are very important for final characteristics and application of PCC. The most widely used PCC surface coating is the treatment with fatty acids, usually stearic acid. As a result, a monolayer of hydrophobic organic molecules is attached to the mineral surface. The structure and properties of such an ultrathin organic film have a strong influence on the final properties of PCC[5].

It is generally accepted that carboxylic acids or their salts react with calcium carbonate to produce a layer of the corresponding calcium salt (calcium stearate in the case of stearic acid) on the surface[6, 7].

It has been found that only one stearic acid molecule is attached to each Ca^{2+} and the alkyl chains in a complete monolayer are vertically oriented to the calcite surface. Also, X-ray scattering confirmed the vertical orientation of the alkyl chains. The thickness of the stearate monolayer was found to be about 2.6 nm which shows the molecular length of stearic acid. The use of excess acid to ensure complete surface reaction, leads to multilayer adsorption in which only a monolayer is chemisorbed while the other is physisorbed in a tail-to-tail arrangement. Therefore, the use of optimal amount of surface modifier is not only of economic importance but also technically advantageous[8, 9]. Figure 3.1 reveals the schematic illustration of interaction between the organic substrate and inorganic mineral in aqueous medium[10].

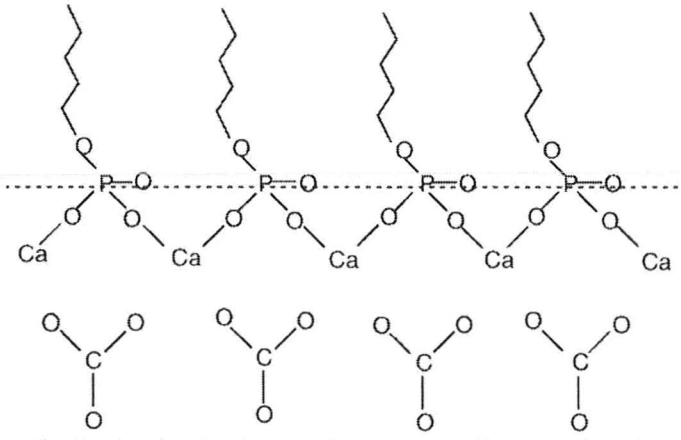

Figure3.1 Schematic illustration for interaction between the organic substrate and calcium carbonate[10]

3.2.2 Colloidal Silica

Spherical, monodisperse particles of colloidal silica can be conveniently prepared by hydrolysis of tetraalkyl orthosilicates according to the Stober method. This process has also attracted attention in ceramics, colloids, and catalysis[11, 12].

The study of colloidal silica is motivated by the remarkably interesting properties that they possess and wide variety of industrial applications. Having colloidally stable silica in a variety of solvents with different polarity based on electrostatic, steric, or electrosteric forces was always very interesting. The ideal colloidal silica is monodisperse with appropriate functional groups that can freely react with other moieties to be prepared or modified[13].

As mentioned earlier, one well-studied colloidal system which has widespread use in several areas is colloidal silica prepared by the Stober process. The process involves the ammonia-catalyzed hydrolysis and condensation of tetraethyl orthosilicate (TEOS) [14].

This process has several characteristics as below[15]:

- The particles can be grown to diameters in the range of 20 nm to 1 micrometer.
- Colloidally stable spherical particles with narrow size distribution.
- Limited porosity of colloidal silica particles.
- Possible chemical modification of the surface of the particles

Stober silica is electrostatically stabilized by the electrical double layer formed from the ionization of silanol groups which is facilitated by the presence of the aqueous NH_3 mixture.

3.3 EXPERIMENTAL

***Materials*:** Commercial grades of precipitated calcium carbonates (PCC) were Socal 31 (Solvay), Ultra Pflex and Thixo-Carb HP (Specialty Minerals). The parameters of PCC samples are summarized in Table 3.1.

Table 3.1 Characteristics of commercial PCCs

Name	*Specific surface area (m^2/g)*	*Average particle size (nm)*	*Stearic acid content (%)*
Socal 31	20	70	0
Thixo-Carb HP	28	60	2.5
Ultra Pflex	19	70	3

Stearic acid with molecular weight of 284.48 and glass beads with 106 μm mean particle size were purchased from Sigma Aldrich. Reagent grade Ethylenediaminetetraacetic acid (EDTA) was purchased from J.T. Baker. An acidic, aqueous dispersion of colloidal silica stabilized with aluminum oxide (Bindzil CAT 80) were prepared from AkzoNobel without further cleaning or purification.

3.3.1 Treatment with stearic acid

The untreated commercial PCC samples were acid treated in the lab to be hydrophobic. In this method, a very thin monolayer of hydrophobic fatty acid is attached to the calcium carbonate surface and the acid group in the fatty acid molecule forms a

water insoluble calcium salt. Then, the hydrophobic tail is oriented to the air and results in a hydrophobic modified PCC with a fatty acid.

Furthermore, by increasing the concentration of fatty acid, the hydrophobicity of PCC increased, until the formation of a bilayer adsorption of fatty acid on PCC where the extra hydrophobic tails of fatty acid presented on the coating layer and hydrophilic heads orient to the water and results in decreased hydrophobicity.

In this work, 20 g dry powder of untreated PCC (Socal 31) and 0.1 g and 0.2 g stearic acid were mixed into 80 ml of distilled water at 75 °C and 800 rpm mixing rate for 30 minutes to have 0.5% and 1% stearic acid treated PCC. Then, the slurries were dried in the oven (at 105°C for 10 hours) and ground.

3.3.2 Dispersion of PCC in water

To have a lower interaction of PCC particles with each other, 1% solid content dispersions were prepared by adding 1 g PCC to 99 ml distilled water. The dispersions were mixed in 800 rpm shear rate for 12 hours.

3.3.2 Electrophoresis

Electrophoretic mobilities were measured at 25°C with a Brookhaven Zetapals Microelectrophoresis apparatus in the phase analysis light scattering mode using BIC Pals Zeta Potential Analyzer software version 2.5. Measurements were repeated 3 times.

3.3.3 Dynamic Light Scattering (DLS)

DLS was employed to determine the particle size distribution of PCC and colloidal silica particles. When light hits small particles, the light scatters in all directions so long as the particles are small compared to the wavelength (below 250 nm). If the light source is a laser, and thus is monochromatic and coherent, then one observes a time-dependent fluctuation in the scattering intensity. These fluctuations are due to the fact that the small molecules in solutions are undergoing Brownian motion and so the distance between the scatterers in the solution is constantly changing with time. This scattered light then undergoes either constructive or destructive interference by the surrounding particles and within this intensity fluctuation, information is contained about the time scale of movement of the scatterers.

There are several ways to derive dynamic information about particles' movement in solution by Brownian motion. One such method is dynamic light scattering, also known as quasi-elastic laser light scattering. The dynamic information of the particles is derived from an autocorrelation of the intensity trace recorded during the experiment. The second order autocorrelation curve is generated from the intensity trace.

Dynamic light scattering provides insight into the dynamic properties of soft materials by measuring single scattering events, meaning that each detected photon has been scattered by the sample exactly once. However, the application to many systems of scientific and industrial relevance has been limited due to often-encountered multiple scattering, wherein photons are scattered multiple times by the sample before being detected. Accurate interpretation becomes exceedingly difficult for systems with non-negligible contributions from multiple scattering. Particularly for larger particles and

those with high refractive index contrast, this limits the technique to very low particle concentrations, and a large variety of systems are, therefore, excluded from investigations with dynamic light scattering. However, it is possible to suppress multiple scattering in dynamic light scattering experiments via a cross-correlation approach. The general idea is to isolate singly scattered light and suppress undesired contributions from multiple scattering in a dynamic light scattering experiment. Different implementations of cross-correlation light scattering have been developed and applied. Currently the most widely used scheme is the so called 3D-dynamic light scattering method.

3.3.4 Contact Angle measurement

Contact angle measurement (CA) was employed to analyse the hydrophobicity of the samples. The contact angle is the angle between the tangent line and the solid surface when drawing a tangent line from the droplet to the touch of the solid surface.

In order to measure the hydrophobicity of stearic acid treated PCC samples, PCC powders were pressed to have a smooth surface and the contact angle between water droplets and PCC surface was measured.

3.3.5 Titration

In order to evaluate how much PCC dissolved in water, titration was carried out (Man _Tech PC Titrate). Despite the fact that titration is time consuming the titration method is the most precise method to measure calcium ions in the solution. EDTA was utilized as titrant to determine dissolved PCC.

EDTA is a weak acid that can lose four protons on complete neutralization. Its structural formula is shown in Figure 3.2.

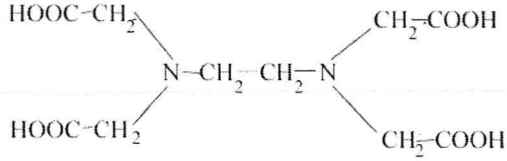

Figure3.2 Chemical structure of EDTA

Four acid sites and two nitrogen atoms all contain unshared electron pairs, so that a single EDTA ion can form a complex with six sites on a cation. This complex is stable with EDTA and the metal ion in a 1:1 mole ratio. Also, the conditions of its formation can be controlled.

3.3.6 Scanning electron microscopy (SEM)

SEM was employed to study the deposition of PCC and silica particles as collectors onto the glass beads. Also, SEM can support the result of particle size obtained from DLS.

3.3.7 Flotation

The flotation tests were carried out with a laboratory bench scale flotation device which is schematically showed in Figure 3.3.

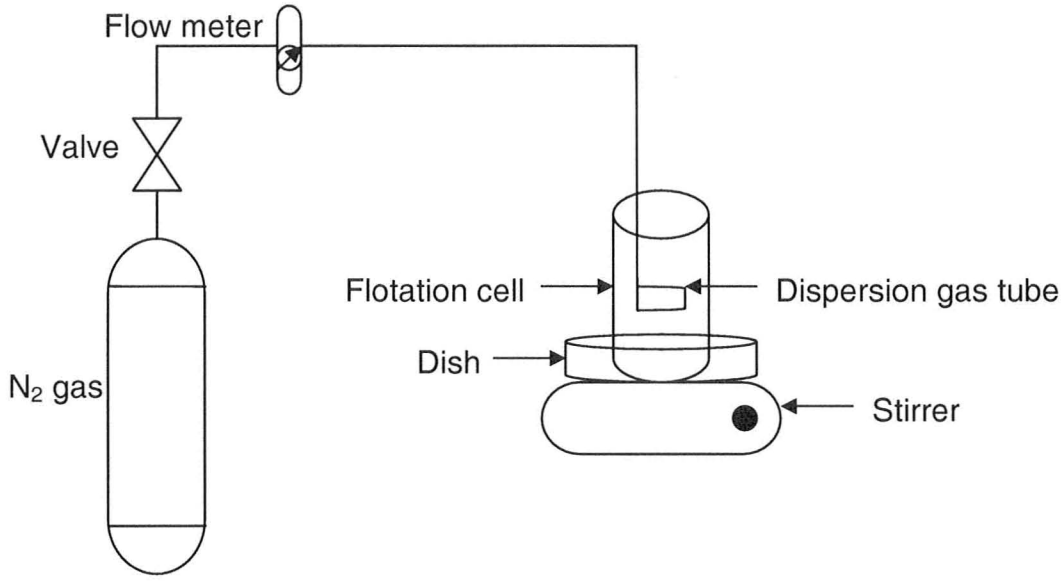

Figure3.3 Schematic picture of experimental set up for laboratory flotation

Flotation procedures were carried out at pH 9 and 5 mM NaCl solution was used in all experiments to adjust the solution ion strength. First, glass beads (1 g) and PCC (0.02, 0.05, and 0.1 g) were mixed with each other. This step is conditioning time. Conditioning time for all flotation tests was 5 min. After conditioning time, frother was added to make bubbles stable. The frother used was MIBC (Methyl Isobuthyl Carbinol). In order to make bubble, nitrogen gas was applied to the flotation cell through dispersion gas tube. The pressure of nitrogen gas applied was constant during the whole experiment and also for all flotation experiments. The froth came up the beaker was scraped with a ruler every 5 seconds. Therefore, we could collect the glass beads extracted from the flotation bath in different dishes. In order to have constant amount of water during the experiment, the water was added to the bath between any dishes. Also, MIBC lost was calculated based on the amount of water lost. In this way, three concentrates were collected at 1.5, 3, and 4.5 minutes by scraping the froth into three dishes. The recovery percentage was measured by filtering, drying, and weighing the concentrates. The ratio between the weights of the final extracted glass beads with flotation to the input glass beads is recovery percentage.

3.4 RESULTS AND DISCUSSION

3.4.1 Mean particle size and mobility

Mean particle size and mobility of all dispersions were determined and the results are listed in Table 3.2. All samples are in 5 mM NaCl solution at pH 9.

Table3.2 Mean particle size and mobility of different PCC dispersions

	Mean particle size (D50%) (μm)	*Mobility* $((m^2/Vs)*10^{-8})$
Untreated PCC (Socal 31)	4.5	1.12
0.5% stearic acid treated PCC	9.4	0.92
1% stearic acid treated PCC	12.3	0.79
2.8% stearic acid treated PCC (Thixo-Carb HP)	20	-0.41

Table 3.2 shows that by increasing the amount of stearic acid, the mean particle size of PCC dispersion increased and mobility and consequently colloidal stability of PCC dispersion diminished.

3.4.2 Water contact angle

In order to evaluate the role of stearic acid percentage on hydrophobicity of PCC, water contact angle measurements have been done. The results are available in table 3.3 and Figure 3.4. It is obvious that by increasing the stearic acid content water contact angle and hydrophobicity increased.

Table 3.3 the influence of stearic acid on water contact angle

	Water Contact Angle (degree)
Untreated PCC (Socal 31)	-
0.5% stearic acid treated PCC	26
1% stearic acid treated PCC	31
2.8% stearic acid treated PCC (Thixo-Carb HP)	70
3% stearic acid treated PCC (Ultra Pflex 100)	140

Water contact angle of untreated PCC was not possible to measure because of high hydrophilicity of this sample and fast spreading of the water droplet to the PCC surface. Also, the 3% stearic acid treated sample was very hydrophobic and was not possible to disperse it in water.

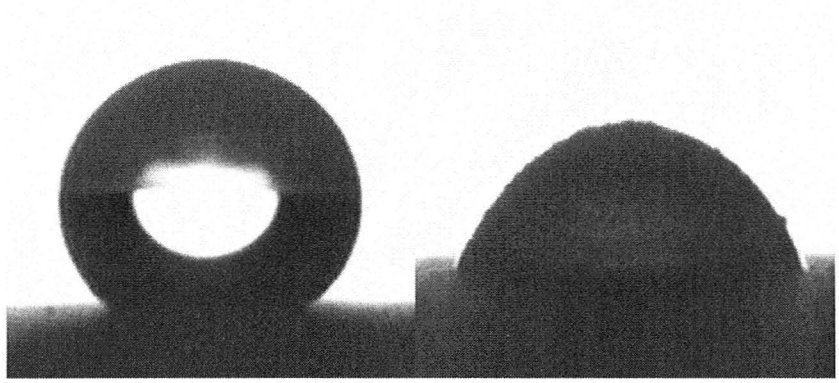

a b

Figure3.4 Water contact angle of a) 3% stearic acid treated and b) 2.5% stearic acid treated samples

3.4.3 Titration

In order to evaluate dissolved calcium carbonate in distilled water, titration was carried out for supernatants of 1% PCC dispersions. EDTA was added to the solution and the mV potential recorded. Then, the milliliters of EDTA added to the solution were plotted against the mV potential. The endpoint is the point that potential is constant and does not change any more. Figure 3.5 shows an example of titration PCC with EDTA.

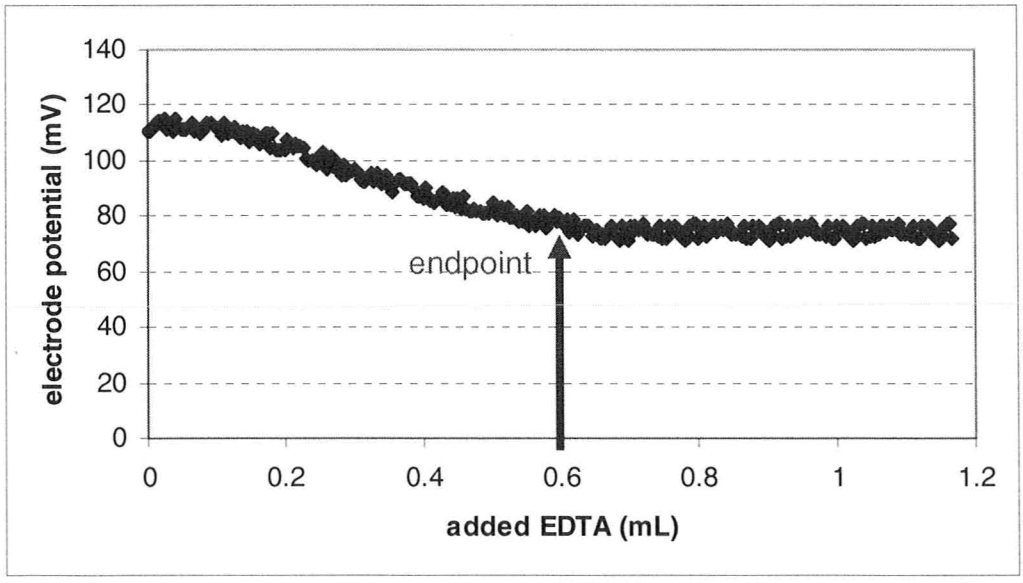

Figure3.5 A sample graph of titration PCC with EDTA

Using the following equation, the amount of calcium ions in the solution was calculated:

$M_{Ca}^{+2} = (V_t M_t)/ (V_{Ca}^{+2})$

M_{Ca}^{+2}: concentration of calcium ion (moles/liter)
V_t: Volume of EDTA added at endpoint
M_t: EDTA concentration (moles/liter)
V_{Ca}^{+2}: volume of the sample

As 1 mole Ca^{2+} titration is equal to 1mole $CaCO_3$ titration, we can convert the calcium ions to calcium carbonate dissolved. The results are listed in Table 3.4.

Table3.4 Calcium ions and calcium carbonate amount dissolved in water

	Ca^{+2} (moles/liter)	*$CaCO_3$ (ppm)*
Untreated PCC	$1.25 * 10^{-4}$	12.5
0.5% stearic acid treated PCC	$7.5 * 10^{-5}$	7.5
1% stearic acid treated PCC	$6.25 * 10^{-5}$	6.25

As we expected, the amount of calcium carbonate dissolved in water are very low and by increasing the hydrophobicity of calcium carbonate becomes less.

3.4.4 Flotation

Flotation experiments were done for all PCC samples and the results are graphed in figure 3.6. The control experiments with no particle show 18% recovery of glass beads.

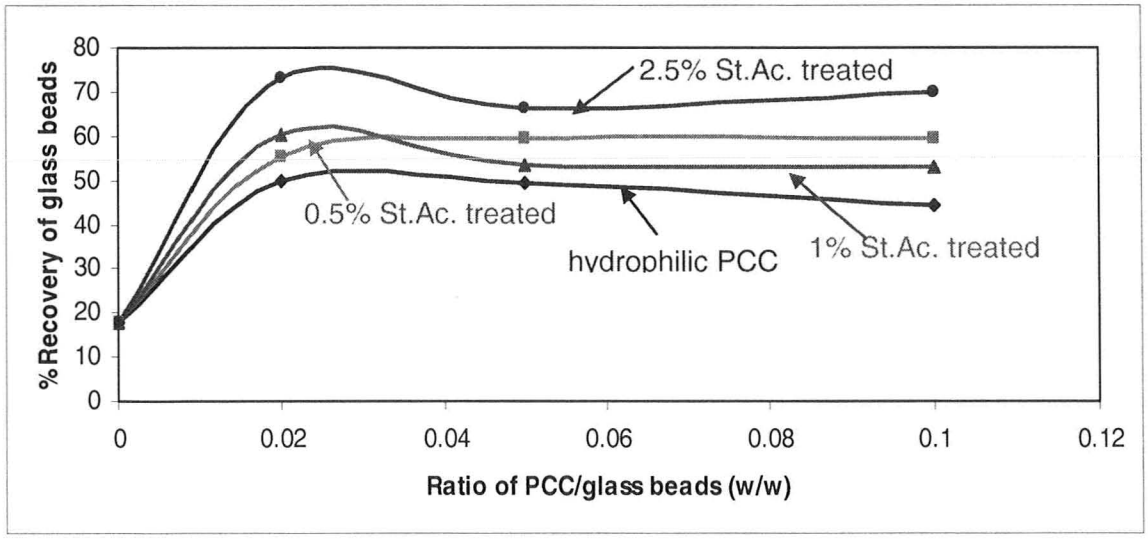

Figure3.6 Flotation of glass beads with different types of PCC

It is clear from graphs that by increasing the percentage of St.Ac. and increasing the hydrophobicity, flotation of glass beads increased. Also, it is obvious that increasing the ratio of PCC to glass beads does not increase the flotation recovery. We believe that

the main problem is particle size of PCC. PCC with big particle size- in micron range- cannot deposit appropriately to the glass beads and take them out of the flotation cell.

3.4.5 SEM

To see deposition of PCC particles to glass beads, SEM experiments have been done. In this method, we can assess how PCC particles attach to glass beads. Figures 3.7 to 3.9 show deposition of different types of PCC to glass beads.

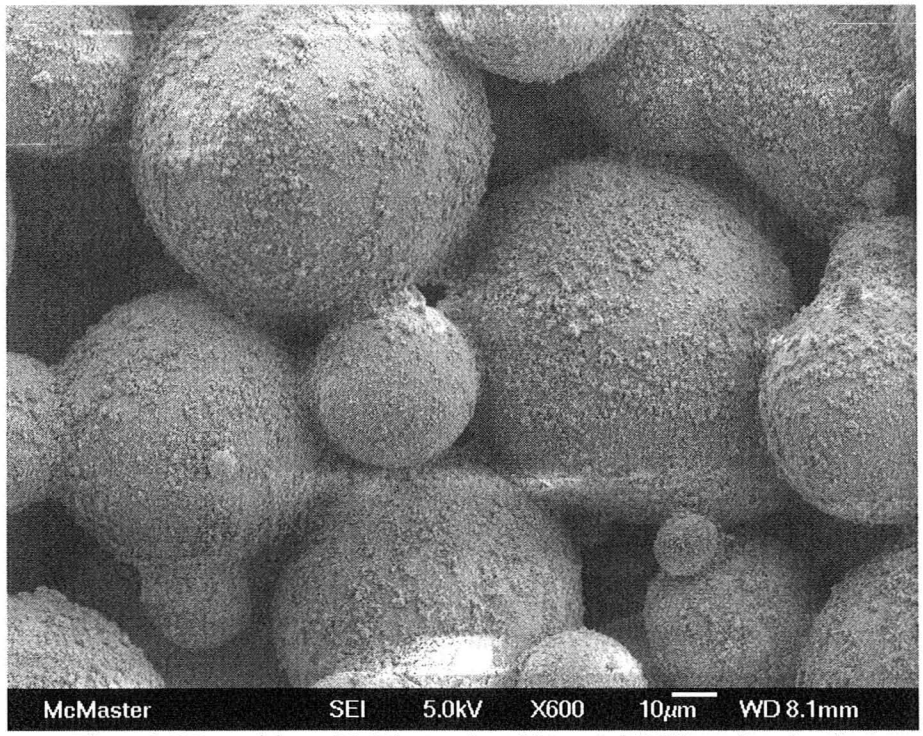

Figure3.7 Deposition of 2.5% stearic acid treated PCC to glass beads

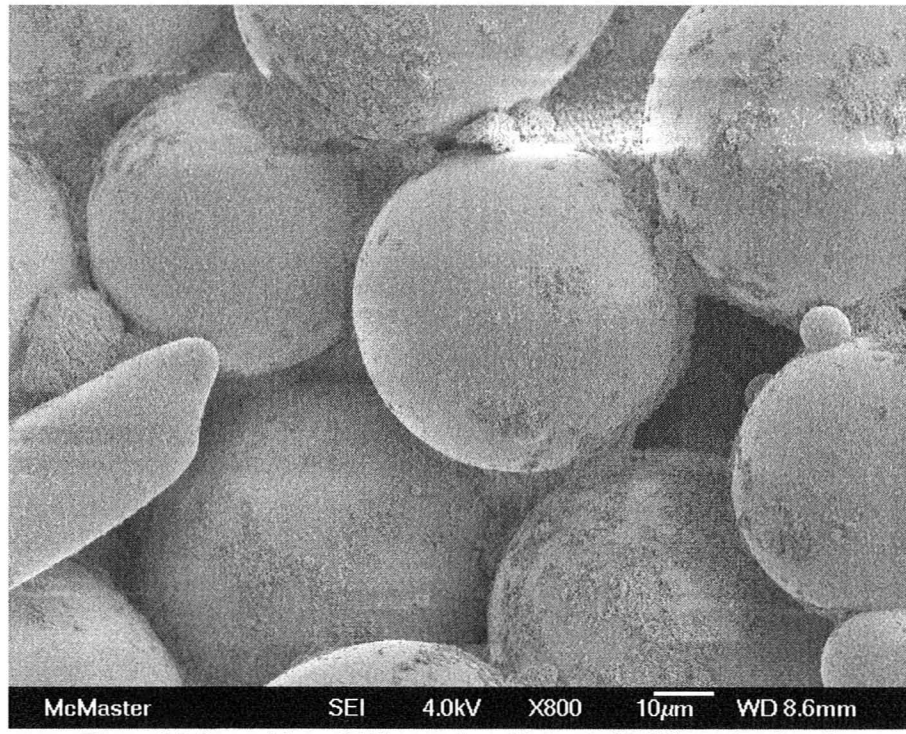

Figure3.8 Deposition of 1% stearic acid treated PCC to glass beads

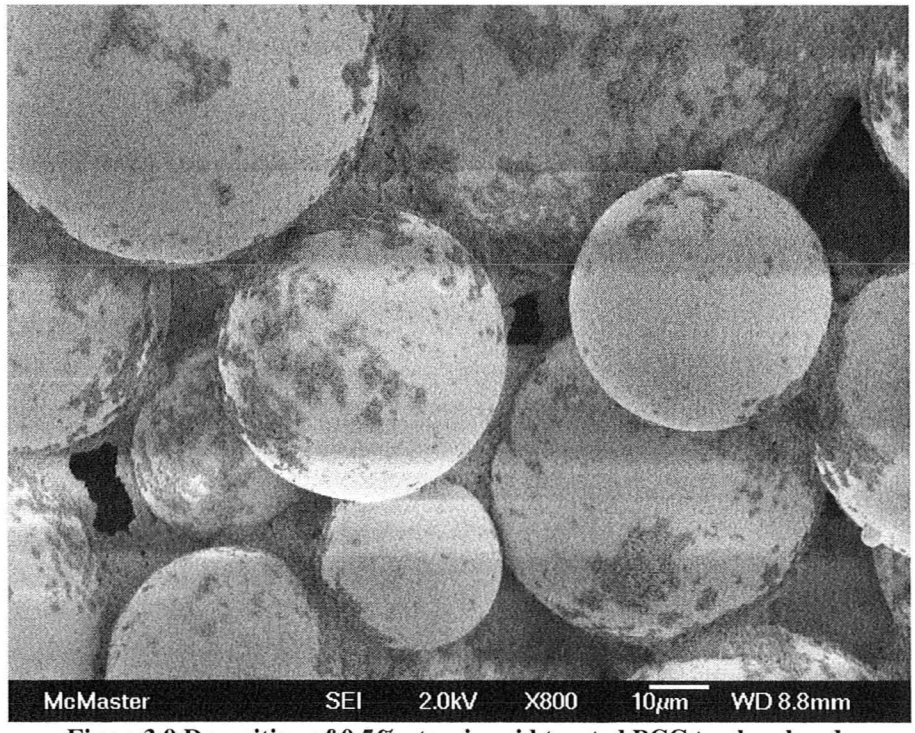

Figure3.9 Deposition of 0.5% stearic acid treated PCC to glass beads

SEM images show poor deposition of PCC samples to glass beads which comes from the size of PCC particles that cannot work satisfactory as collectors for glass beads in when they are in micron range.

3.4.6 Experiments for reduction of the particle size

Many experiments have been performed to decrease the particle sizes to nano scale such as reducing the solid content from 1% solid content to 0.5% solid content, ultrasonication for 30 minutes, and adding Poly sodium 4-styrene-sulfonate as a surfactant. But, none of them decreased the particle size.

Furthermore, in order to stabilize the PCC dispersion in water, the washing process was examined[16]. In this method, PCC particles were dispersed in distilled water and then the dispersions were stocked for 1 week and the supernatants were changed every day. After one week, they dried at 120 °C for 4 hours. Then, 1% solid content dispersion was prepared and stirred at 1000 rpm for 1 h and submitted to ultrasonic at 50 kHz for 15 min and consequently stirred for 3 more hours at 1000 rpm.

In another attempt, high solid method was tried. In this method, 20% poly ethylene glycol (PEG) was added to the water to reduce the interfacial tension. PCC was dispersed at higher solids (20%wt) where mechanical shear can impart significant energy to the dispersion. After that, dispersions were diluted down to the desired solid content.

In other series of experiments, ball mill dispersion was tried in Xerox Company's lab. In this technique, PCC particles were dispersed in distilled water at high solid Content (20%) for 3 hours at high shear rate (1200 rpm) and then ultrasonicated for 15 minutes and finally submitted to the milling for 48 hours with ball mill in Xerox lab. Unfortunately, the particle size did not reduce in all 3 mentioned methods.

3.4.7 Post-hydrophobizing technique

A post-hydrophobizing technique was carried out for in situ hydrophobizing of PCC particles to disperse particles easily in aqueous environment and then make them hydrophobic in flotation cell to deposit to glass beads and air bubbles.

In the conventional method, we made PCC hydrophobic first or used a hydrophobic PCC and then added it to the glass beads in the flotation bath. In this method, first we had conditioning of the glass beads with PCC and then treated PCC particles with different amounts of stearic acid to make them hydrophobic. Flotation results showed no differences for recovery of glass beads in comparison to the conventional method.

3.4.8 Increasing the mobility

It is shown that by increasing the ratio of Ca^{2+} ions in solution, the mobility increases[17]. Therefore, flotation experiments have been done in different concentration of Ca^{2+} ions. The results showed that despite that increasing the concentration of Ca^{2+} ions increases the mobility, but it is not very effective on flotation results. These results of mobility enhancement and flotation are shown in Figures 3.10 and 3.11 respectively.

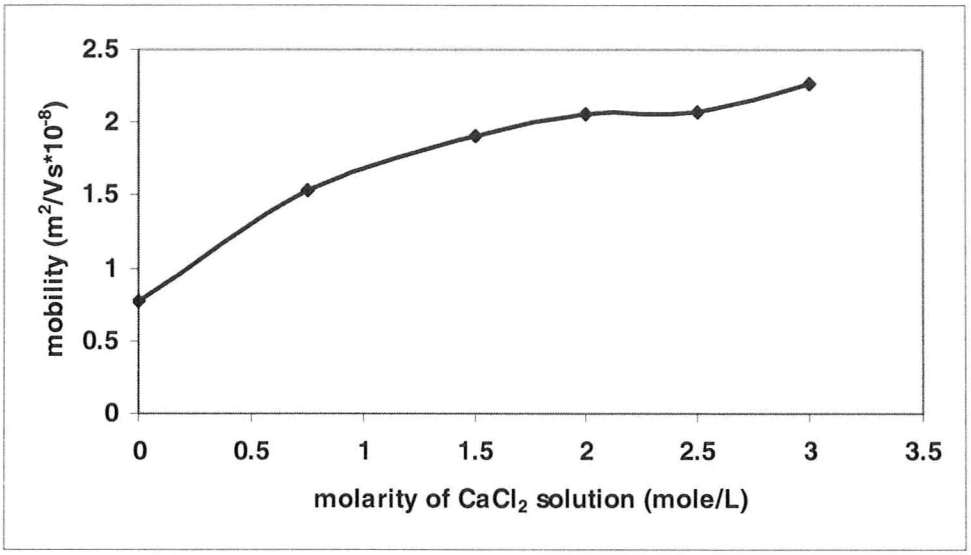

Figure3.10 Mobility of 1% stearic acid treated PCC versus concentration of Ca^{2+}

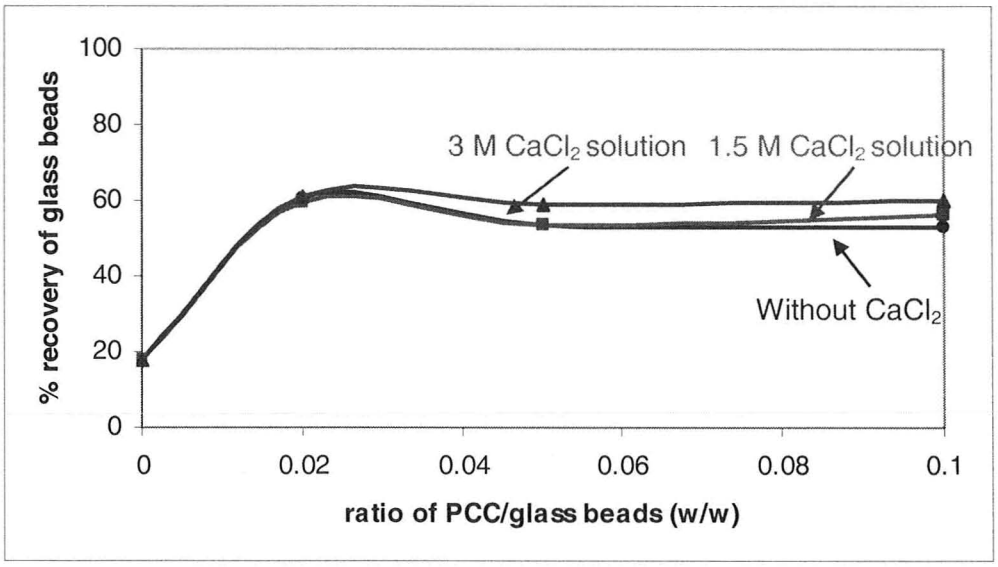

Figure3.11 Flotation of glass beads with 1% stearic acid treated PCC with different concentration of Ca^{2+}

3.4.9 Colloidal Silica

Also, silica nanoparticles were employed as another inorganic nanoparticle for flotation systems. We started with commercial grade silica (Bindzil CAT 80) which is an acidic aqueous dispersion of colloidal silica stabilized with aluminum oxide.

But, this dispersion is stable just at low pHs and by increasing the pH started to aggregate. The behavior of particle size and mobility by increasing the pH is summarized in table 3.5. All measurements carried out in 5 mM NaCl solution.

Table3.5 Behavior of Bindzil CAT 80 based on pH

pH	Mobility (m^2/Vs)*10^{-8})	($Dv_{0.5}$) nm
3.72	4.30	182
4.50	4.31	210
6.0	3.48	157
7.0	3.02	243
8.0	2.38	488
9.0	0.04	16590

Data in table 3.5 show that by increasing the pH, mobility decreases and particle size increases and colloidal stability of dispersion collapses. Besides, this colloidal silica was employed as a collector for flotation of glass beads. The flotation recovery at low pH was very low that could come from hydrophilic nature of silica. The SEM image confirms low deposition of silica to glass beads at low pH.

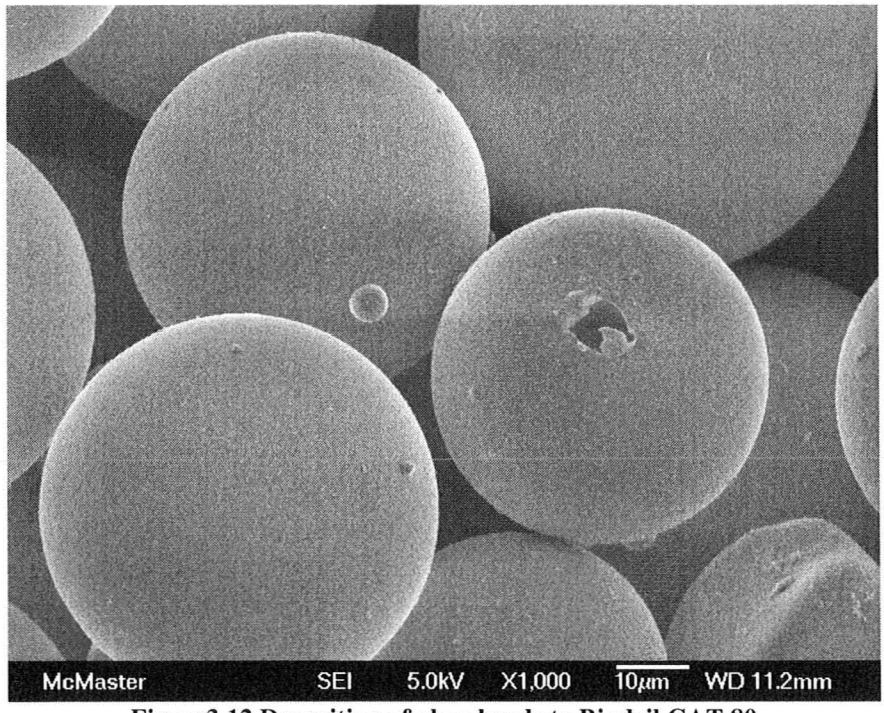

Figure3.12 Deposition of glass beads to Bindzil CAT 80

On the other hand, working at regular pH of flotation (pH 9) resulted in coagulation of silica nanoparticles. Again, flotation recovery of glass beads were low and SEM images show some aggregations of silica on glass beads.

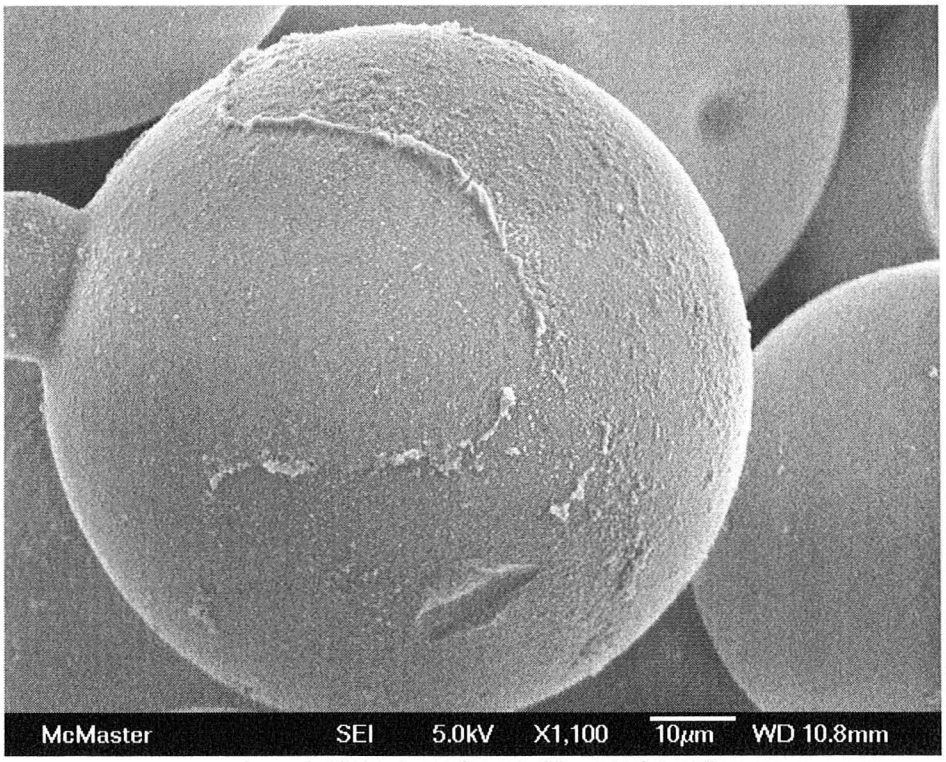

Figure3.13 Aggregation of silica at high pH

3.5 Conclusion

Treatment of PCC with stearic acid was successfully done with attachment of stearic acid molecule to Ca^{2+} and vertically orientation of alkyl chains monolayer which make it hydrophobic. Water contact angle measurements confirm the role of stearic acid content in hydrophobicity.

But, having stable dispersion of PCC in water was not achieved. Despite that commercial PCC samples originally were in nano range, but they coagulated in water to micron range. Different methods have been examined to reduce the particle size of commercial PCC samples which none of them were successful.

Flotation experiments showed low recovery of glass beads when PCC samples were employed as collector. The main reason maybe related to their particle size which prevents them from appropriate deposition to glass beads. SEM images confirmed it.

Also, commercial grade colloidal silica was employed as inorganic nanoparticle collector in flotation of glass beads. The experiments showed that colloidal silica is stable at low pH but by increasing the pH, the particle size increased and colloidal stability decreased.

Recovery percentage of glass beads was low when silica was employed as collector in low and high pH. The main reason could be the hydrophilic character of silica at low pH and its coagulation at high pH.

The results also showed that commercial inorganic nanoparticles are not appropriate collectors for flotation of glass beads. Therefore, inorganic nanoparticles should be prepared and used in theirs dispersed form without any drying and redispersion.

3.6 References:

1. Cho, K.; Saheb, D. N.; Choi, J.; Yang, H., Polymer **2002**, 43, 1407-1416.
2. Lam, T. D.; Hoang, T. V.; Quang, D. T.; Kim, J. S., Mat. Sci. Eng. A **2009**, 501, 87-93.
3. Hu, Z.; Zen, X.; Gong, J.; Deng, Y., Colloids and Surfaces A: Physicochem. Eng. Aspects **2009**, 351, 65–70.
4. Osman, M. A.; Suter, U. W., Chem. Mater. **2002**, 14, 4408-4415.
5. Ashan, T.; Taylor, D. A., J. Adhesion **1998**, 67, 69.
6. Ukrainczyk, M.; Kontrec, J.; Kralj, D., J. Coll. Inter. Sci. **2009**, 329, 89-96.
7. Sutherland, I.; Maton, D.; Harrison, D. L., Chem. Mater. **2002**, 14, 4408-4415.
8. Papirer, E.; Schultz, J.; Turchi, C., Eur. Polym. J. **1984**, 20, (12), 1155.
9. Fekete, E.; Pukansky, B.; Toth, A.; Bertoti, I., J. Colloid Interface Sci. **1990**, 135, (1), 200.
10. Wang, C.; Xiao, P.; Zhao, J.; Zhao, X.; Liu, Y.; Wang, Z., Powder Technology **2006**, 170, 31-35.
11. Badley, R. D.; Ford, W. T.; McEnroe, F. J.; Assink, R. A., Langmuir **1990**, 6, 792-801.
12. Badley, R. D.; Ford, W. T., J. Org. Chem. **1989**, 54, 5437-5443.
13. Pham, K. N.; Fullston, D.; Sagoe-Crentsil, K., Aust. J. Chem. **2007**, 60, 662-666.
14. Stober, W.; Fink, A.; Bohn, E., J. Colloid Interface Sci. **1968**, 26, 62-69.
15. Ketelson, H. A.; Brook, M. A.; Pelton, R. H., Chem. Mater. **1995**, 7, 1376-1383.
16. Antunes, E.; Garcia, F. A. P.; Ferreira, P.; Rasteiro, M. G., Chem. Eng. Research and Design **2008**, 86, 1155-1160.
17. Szczes, A.; Chibowski, E.; Holysz, L., Colloids and Surfaces A: Physicochem. Eng. Aspects **2007**, 297, 14-18.

Chapter 4

Second generation inorganic particles as flotation collectors

4.1 ABSTRACT

Stearic acid treated PCC nanoparticles were synthesized with the carbonation method and characterized with electrophoretic mobility, dynamic light scattering, FTIR and contact angle measurements. The flotation experiments have also been carried out by employing PCC nanoparticles and the results showed high recovery percentage of glass beads.

In another series of experiments, silica nanoparticles have been prepared by the Stober method. Also, they have been modified with aminopropyltriethoxy silane (APTS) and mercaptopropyltrimethoxy silane (MPTS) with three different methods. Characterization experiments confirmed synthesis of silane modified silica nanoparticles.

However, flotation results of glass beads when APTS modified silica nanoparticles employed as collector are not very satisfactory which can be related to their hydrophilic characteristics.

4.2 INTRODUCTION

4.2.1 Synthesis of Precipitated Calcium Carbonate (PCC)

There are lots of industrial applications for PCC such as composites, plastics, textiles, rubber, paints and paper. These industrial applications need PCC particles with excellent properties. The properties such as narrow size distribution, uniform shape, and definite crystal structure play a crucial role in PCC properties. In this way, the method of production and the process parameters are critical[1].

Recently, using nanosized PCC particles has become very attractive for various industries because of their properties. Therefore, synthesis of nano-PCC is being given more and more attention[2].

Synthesis of calcium carbonate was followed by two basic synthetic routes: the solution route and the carbonation method[3]. The carbonation process is usually used in industry due to its low cost and the availability of the raw materials. This process often includes the calcination of the limestone to produce calcium oxide, the mixing of the

oxide with water to form $Ca(OH)_2$ slurry, and the precipitation of $CaCO_3$ via carbonation of $Ca(OH)_2$ slurry with carbon dioxide[4].

The morphology and size of calcium carbonate particles depend mainly on the precipitation condition, such as the carbonation solution and the dispersion of CO_2[5]. In fact, morphological change of calcium carbonate attributed to the supersaturation level, temperature and pH of solution. Also, the crystalline form and particle size distribution are dependent on ionic ratio of $[Ca^{2+}]$ / $[CO_3^{2-}]$ in solution. Although several papers have been published about precipitation of PCC, the relationship between precipitation conditions and final properties of product is still a major challenge[4].

One method for the synthesis of nano-PCC is the synthesis of nanosized surface modified PCC particles using the carbonation method with a surface modifier (fatty acid) simultaneously which is shown in Figure 4.1[6].

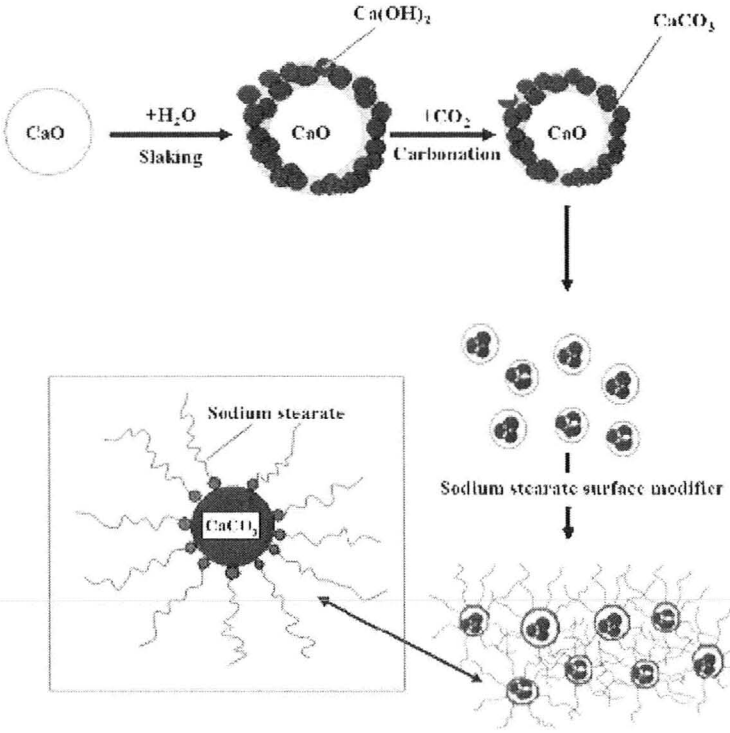

Figure4.1 Synthesis procedure of nanosized surface modified PCC[6]

4.2.2 Modification of colloidal silica nanoparticles using silane coupling agents

Colloidal silica particles have been used in a wide range of applications in ceramics, colloids and catalysis. In almost all cases, the benefit of smaller-sized particles can only be realized if the particles are well dispersed. This is usually achieved by modifying the surface of silica particles with an organosilane to improve the stability[7].

However, the complex surface chemistry of silica tends to destabilize especially for small particles with high specific surface area and most of surface modification methods resulted in aggregation especially for small particles[8, 9].

In fact, silica particles exhibit different dispersion and aggregation behaviors owing to different structures of surface silanol groups. The surface of small silica particles with diameter below 30 nm contains mostly isolated silanol groups owing to the high surface coverage[10].

Generally, colloidal suspensions are considered stable when thermal energy is larger than interparticle attractive forces. Depending on the nature and strength of interparticle forces, particles in an unstable suspension can either coagulate into relatively compact aggregates or flocculate together to form an open network throughout the suspension volume which is known as a colloidal gel[11].

However, there are two common methods for the modification of silica:

- Post-modification (grafting) which is subsequent grafting organo functional alkoxysilane onto colloidal nanosilica.
- In situ modification (co-consideration method) which is simultaneously modification of silica via preparation of colloidal nanosilica using silane coupling agents[12].

There are a few works on the preparation of nanoparticles via the co-condensation method. On the other hand, post-modification is commonly used for modification purpose. However, there are some drawbacks in this method such as reduction of porosity via attaching of organic group to the pore surface and wall, and blocking via diffusion of modifier into the pore for mesoporous silica, multiple reactions, time and energy consuming and the use of organic solvents for silica nanoparticles[13].

4.3 EXPERIMENTAL

***Materials*:** Calcium oxide (CaO) was supplied by Fisher Scientific and stearic acid, glass beads and sodium hydroxide (NaOH) were purchased from Sigma Aldrich to synthesize precipitated calcium carbonate (PCC) nanoparticles. Also, tetraethyl orthosilicate (TEOS), aminopropyltriethoxy silane (APTS) and mercaptopropyltrimethoxy silane (MPTS), ammonia, acetone and methanol were purchased from Sigma Aldrich for the synthesis and functionalization of colloidal silica nanoparticles.

4.3.1 Synthesis of stearic acid treated PCC

0.001 mol of stearic acid ($C_{17}H_{35}COOH$) was added into 100 ml distilled water at 80°C to form the suspension. Then, 0.001 mol NaOH was introduced into the suspension and stirred vigorously for 30 minutes to form sodium stearate.

0.1 mol of CaO was dispersed in 100 ml of distilled water at ambient temperature for 1 hour to form a calcium hydroxide $Ca(OH)_2$ slurry. Then, the slurry was added into the sodium stearate solution synthesized above at 80°C for 3 hours in order for calcium ions of $Ca(OH)_2$ to react with sodium stearate.

Finally in the synthesis of calcium carbonate, the carbonation of the mixture was carried out as mentioned above by bubbling CO_2/N_2 gas mixture with a molar ratio of 3:10. The carbonation reaction should be controlled by the pH value and stopped when the final pH value of suspension reached about 7. The suspension was centrifuged and redispersed in 5 mM NaCl solution at 1% (w/w) solid content under vigorous stirring and sonication.

4.3.2 Synthesis of colloidal silica nanoparticles

The synthesis of silica nanoparticles was performed using the Stober procedure. 2.4 ml TEOS was added via a syringe into a mixture of 80 ml ammonia (28%) and 56 ml methanol. After 30 min sonication, the system was left for 5 hours under nitrogen atmosphere at 30°C. The resulting particles were first washed with methanol using three centrifugation/redispersion cycles using acetone. Then, the silica nanoparticles were dispersed in 5 mM NaCl solution under vigorous stirring and sonication[14].

4.3.3 Preparation of silane-functionalized silica in solvent solution with post-modification method

Aminopropyltriethoxy silane (APTS) was prehydrolized in a methanol: water (3:1) mixture for a few minutes under stirring. Then, silica nanoparticles were reacted with hydrolyzed APTS (Silane: Silica 1:100 and 2:100) in 60 ml toluene for 24 hours at 80°C under nitrogen atmosphere and reflux. The resulting silica-NH_2 particles were washed with methanol and acetone sequentially by using six centrifugation/redispersion cycles and then redispersed in 5 mM NaCl solution under vigorous stirring and sonication. The same procedure was carried out for Mercaptopropyltrimethoxy silane (MPTS) [15].

4.3.4 Preparation of silane-functionalized silica in aqueous solution with post-modification method

In this method, the same solvent solution procedure was employed where APTS was prehydrolyzed in a methanol: water (3:1) mixture for a few minutes under stirring. Then, silica nanoparticles and prehydrolyzed APTS solution were mixed (Silane: Silica 1:100 and 2:100) for 24 hours at 80°C under nitrogen atmosphere and reflux while stirring vigorously. The silica-NH_2 particles were then washed by repeated centrifugation and replacement of supernatant five times. Then, amino silica nanoparticles were redispersed in 5 mM NaCl solution under vigorous stirring and sonication. The same procedure was carried out for MPTS [16].

4.3.5 Preparation of silane-functionalized silica in solvent solution with co-condensation method

In this method, first, 2.4 ml TEOS was added via a syringe into a mixture of 80 ml ammonia (28%) and 56 ml methanol. After 30 min sonication, the system was left for 5 hours under nitrogen atmosphere at 30°C. Then, prehydrolyzed APTS solution were mixed (Silane: Silica 2:100) for 24 hours at 80°C under nitrogen atmosphere and reflux while stirring vigorously. The resulting silica-NH_2 particles were washed with methanol

and acetone sequentially by using six centrifugation/redispersion cycles and then redispersed in 5 mM NaCl solution under vigorous stirring and sonication [17].

4.3.6 Electrophoresis

Electrophoretic mobilities were measured at 25°C with a Brookhaven Zetapals Microelectrophoresis apparatus in the phase analysis light scattering mode using BIC Pals Zeta Potential Analyzer software version 2.5. Measurements were repeated 3 times.

4.3.7 Dynamic Light Scattering (DLS)

DLS was employed to determine the particle size distribution of PCC and colloidal silica particles. When light hits small particles, the light scatters in all directions so long as the particles are small compared to the wavelength (below 250 nm). If the light source is a laser, and thus is monochromatic and coherent, then one observes a time-dependent fluctuation in the scattering intensity. These fluctuations are due to the fact that the small molecules in solutions are undergoing Brownian motion and so the distance between the scatterers in the solution is constantly changing with time. This scattered light then undergoes either constructive or destructive interference by the surrounding particles and within this intensity fluctuation, information is contained about the time scale of movement of the scatterers.

There are several ways to derive dynamic information about particles' movement in solution by Brownian motion. One such method is dynamic light scattering, also known as quasi-elastic laser light scattering. The dynamic information of the particles is derived from an autocorrelation of the intensity trace recorded during the experiment. The second order autocorrelation curve is generated from the intensity trace.

Dynamic light scattering provides insight into the dynamic properties of soft materials by measuring single scattering events, meaning that each detected photon has been scattered by the sample exactly once. However, the application to many systems of scientific and industrial relevance has been limited due to often-encountered multiple scattering, wherein photons are scattered multiple times by the sample before being detected. Accurate interpretation becomes exceedingly difficult for systems with non-negligible contributions from multiple scattering. Particularly for larger particles and those with high refractive index contrast, this limits the technique to very low particle concentrations, and a large variety of systems are, therefore, excluded from investigations with dynamic light scattering. However, it is possible to suppress multiple scattering in dynamic light scattering experiments via a cross-correlation approach. The general idea is to isolate singly scattered light and suppress undesired contributions from multiple scattering in a dynamic light scattering experiment. Different implementations of cross-correlation light scattering have been developed and applied. Currently the most widely used scheme is the so called 3D-dynamic light scattering method.

4.3.8 Contact Angle measurement

Contact angle measurement (CA) is employed to analyse the hydrophobicity of the samples. The contact angle is the angle between the tangent line and the solid surface when drawing a tangent line from the droplet to the touch of the solid surface.

4.3.9 Fourier Transform Infrared Spectrometry (FTIR)

In infrared spectroscopy, IR is radiated through the sample. Consequently, some of the infrared radiation is absorbed by the sample and some is passed through and transmitted. The spectrum resultant is the molecular adsorption and transmission which is unique for each molecular structure similar to a finger print. This makes FTIR spectroscopy useful for several types of analysis.

4.3.10 Si-NMR

NMR is a technique which exploits the magnetic properties of certain nuclei. In principle, NMR is applicable to any nucleus possessing spin. It can be applied to a wide variety of samples, both in the solution and the solid state. When place a sample in a magnetic field, NMR active nuclei absorb at a frequency characteristic of the isotope. The chemical shift reports as a relative measure from reference resonance frequencies which commonly are ^{1}H, ^{13}C, and ^{29}Si. This difference between the frequency of the signal and the frequency of the reference is divided by frequency of the reference signal to give the chemical shift.

4.3.11 Flotation

Flotation procedures were carried out at pH 9 and 5 mM NaCl solution was used in all experiments to adjust the solution ion strength. First, glass beads (1 g) and PCC (0.02, 0.05, and 0.1 g) were mixed with each other. This step is conditioning time. Conditioning time for all flotation tests was 5 min. After conditioning time, frother was added to make bubbles stable. The frother used was MIBC (Methyl Isobuthyl Carbinol). In order to make bubble, nitrogen gas was applied to the flotation cell through dispersion gas tube. The pressure of nitrogen gas applied was constant during the whole experiment and also for all flotation experiments. The froth came up the beaker was scraped with a ruler every 5 seconds. Therefore, we could collect the glass beads extracted from the flotation bath in different dishes. In order to have constant amount of water during the experiment, the water was added to the bath between any dishes. Also, MIBC lost was calculated based on the amount of water lost. In this way, three concentrates were collected at 1.5, 3, and 4.5 minutes by scraping the froth into three dishes. The recovery percentage was measured by filtering, drying, and weighing the concentrates. The ratio between the weights of the final extracted glass beads with flotation to the input glass beads is recovery percentage.

4.4 RESULTS AND DISCUSSION

4.4.1 Characterization of PCC nanoparticles

4.4.1.1 Mean particle size and mobility of PCC

The mobility and mean particle size of PCC dispersion were examined and summarized in Table 4.1.

Table4.1 Properties of PCC dispersion

Solid Content	1 wt% in 5 mM NaCl solution
pH	7.15
Particle Size (nm)	231
Mobility ($(m^2/Vs)*10^{-8}$)	0.82

Table 4.1 shows that PCC particles are well dispersed in aqueous media. Repeating these experiments after 14 days shows stability of PCC dispersion.
The spectra of lab synthesize PCC is the same as commercial stearic acid treated sample.

4.4.1.2 FTIR experiments of PCC samples

To assess PCC samples and characterize chemical bonds, FTIR experiments have been done on commercial PCC grade (Ultra Pflex from Specialty Minerals) and lab prepared sample which can be seen in Figure 4.2.

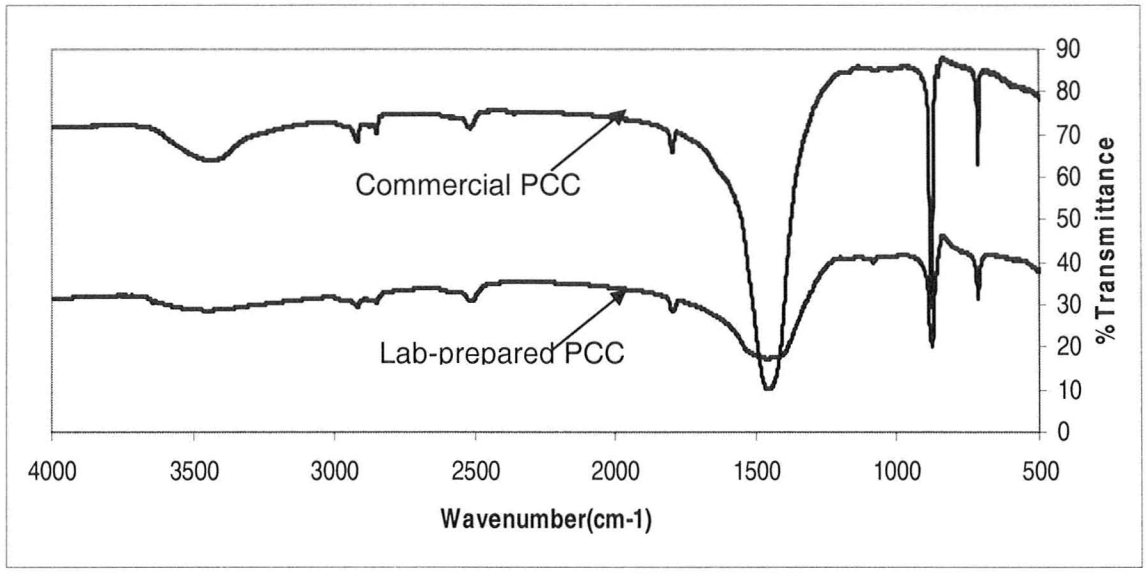

Figure4.2 FTIR spectra of lab synthesize and commercial PCC particles

Based on Figure 4.2, the commercial and lab prepared calcium carbonates show strong peaks in IR spectrum at 1430, 872 and 712 cm^{-1} attributable to the vibration of C=O in the carbonate ion[18]. Also, absorption around 2920 and 2850 cm-1 characterized as H-C-H asymmetric and symmetric stretching vibration respectively. Broad and weak vibration at 3400-3500 is assigned to OH stretching of water[6, 19].

4.4.1.3 Water contact angle

In order to evaluate the hydrophobicity of PCC, water contact angle measurement of stearic acid treated calcium carbonate nanoparticles has been done. The result is shown in Figure 4.3.

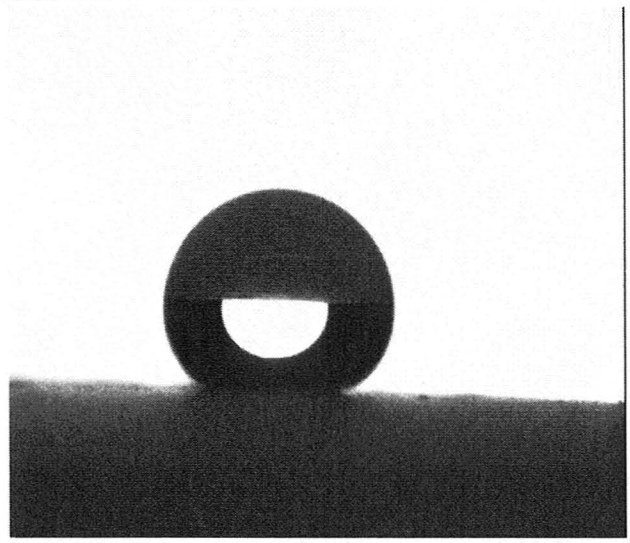

Figure4.3 Water contact angle of lab prepared PCC particle

The water contact angle results confirm hydrophobicity of calcium carbonate. The contact angle between water droplet and PCC surface is about 110 degrees.

4.4.1.4 Flotation by employing PCC nanoparticles

Flotation of glass beads have been done by employing PCC nanoparticles as collectors. Results are shown in Figure 4.4.

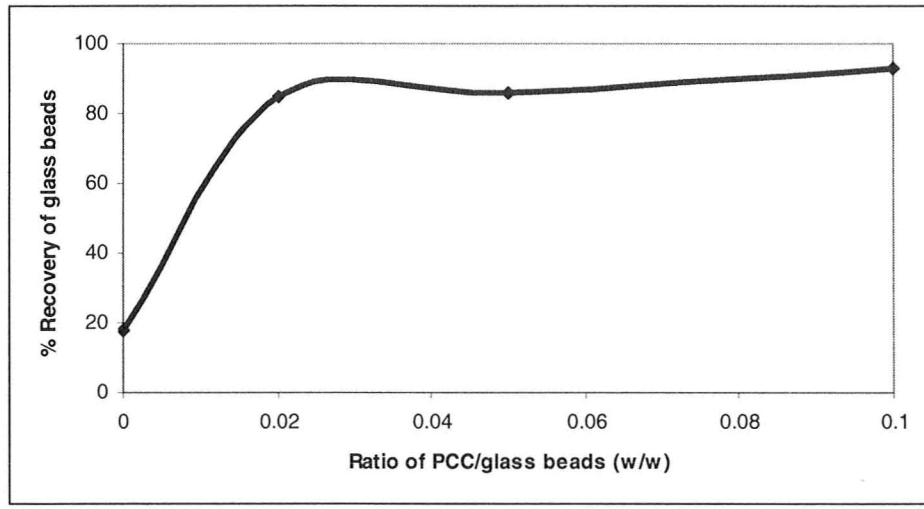

Figure4.4 Flotation of glass beads with stearic acid treated PCC nanoparticle

Figure 4.4 shows that employing hydrophobic PCC nanoparticles as flotation collectors works very well. PCC nanoparticles deposit to glass beads appropriately and increase the recovery percentage to an acceptable range (more than 90%). This result confirms that by reducing the particle size of PCC particles, they show good flotation recovery percentage.

4.4.2 Characterization of silica nanoparticles

4.4.2.1 Mean particle size and mobility of silica nanoparticles

Mean particle size and mobility of colloidal silica nanoparticles were determined and the results are listed in Table 4.2.

Table4.2 Properties of silica nanoparticles

Solid Content	1 wt% in 5 mM NaCl solution
pH	7.05
Particle Size (nm)	92.7
Mobility ($(m^2/Vs)*10^{-8}$)	-3.04

Table 4.2 confirms that colloidal silica particles are in nano range and negatively charged in natural pH.

4.4.2.2 Solid state ^{29}Si NMR

Solid state ^{29}Si NMR was carried out on silica nanoparticles. Two intense signals at -109.25 and -101.52 ppm and a weak signal at -92.31 were characterized which are known as Q_4, Q_3, Q_2 and related to (Si-O-Si), Si(OH) and $Si(OH)_2$ groups[15]. Figure 4.5 shows NMR graph.

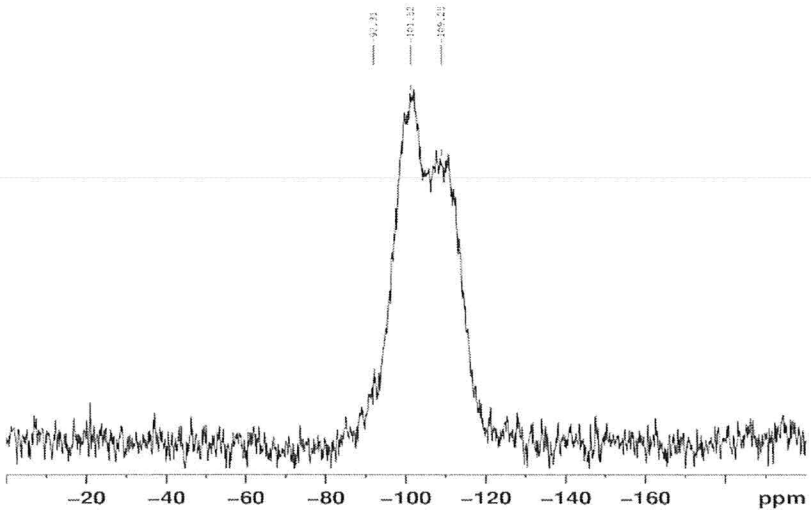

Figure4.5 Solid state ^{29}Si NMR of Stober silica

4.4.2.3 Mean particle size and mobility of silane-functionalized silica in solvent solution with post-modification method

Table 4.3 summarized the mobility and particle size results of silica nanoparticles which are functionalized with different amount of APTS and MPTS.

Table4.3 Properties of silane functionalized silica nanoparticles in solvent solution

	APTS		MPTS	
Solid Content	1 wt% in 5 mM NaCl solution	1 wt% in 5 mM NaCl solution	1 wt% in 5 mM NaCl solution	1 wt% in 5 mM NaCl solution
pH	7.8	7.8	7.1	7.1
Silane: Silica	1:100	2:100	1:100	2:100
Particle Size (nm)	94.4	102.9	89.7	124.1
Mobility $((m^2/Vs)*10^{-8})$	-1.53	-0.74	-0.26	-0.53

Table 4.3 shows the effect of silane percentage on particle size of the silica nanoparticle. The particle size increased with increasing the ratio of silane: silica. This is due to the increase in concentration of functional groups which consequently induces the growth of the particles.

4.4.2.4 Mean particle size and mobility of silane-functionalized silica in aqueous solution with post-modification method

The properties of silane treated silica nanoparticles in aqueous solution have been summarized in Table 4.4.

Table4.4 Properties of silane functionalized silica nanoparticles in aqueous solution

	APTS	MPTS
Solid Content	1 wt% in 5 mM NaCl solution	1 wt% in 5 mM NaCl solution
pH	8	7.8
Silane: Silica	2:100	2:100
Particle Size (nm)	140.8	175.6
Mobility $((m^2/Vs)*10^{-8})$	-1.23	-5.32

4.4.2.5 Mean particle size and mobility of silane-functionalized silica in solvent solution with co-condensation method

Also, properties of MPTS functionalized silica nanoparticles with co-condensation method have been studied. The silane: silica ratio is 2:100. As you can see in Table 4.5, the mean particle size is very similar to the particle size of silica synthesized with post modification method. However, the mobility is much lower than the former method.

Table4.5 Properties of silane functionalized silica nanoparticles with co-condensation method

Solid Content	1 wt% in 5 mM NaCl solution
pH	7.55
Particle Size (nm)	127.6
Mobility ($(m^2/Vs)*10-8$)	-2.21

4.4.2.6 FTIR experiments on silica and silane treated silica nanoparticles

The functional groups in the amino silane treated samples were identified by FTIR data of silane functionalized silica nanoparticle. Figure 4.6 shows FTIR spectra of the resulting silane modified silica nanoparticles.

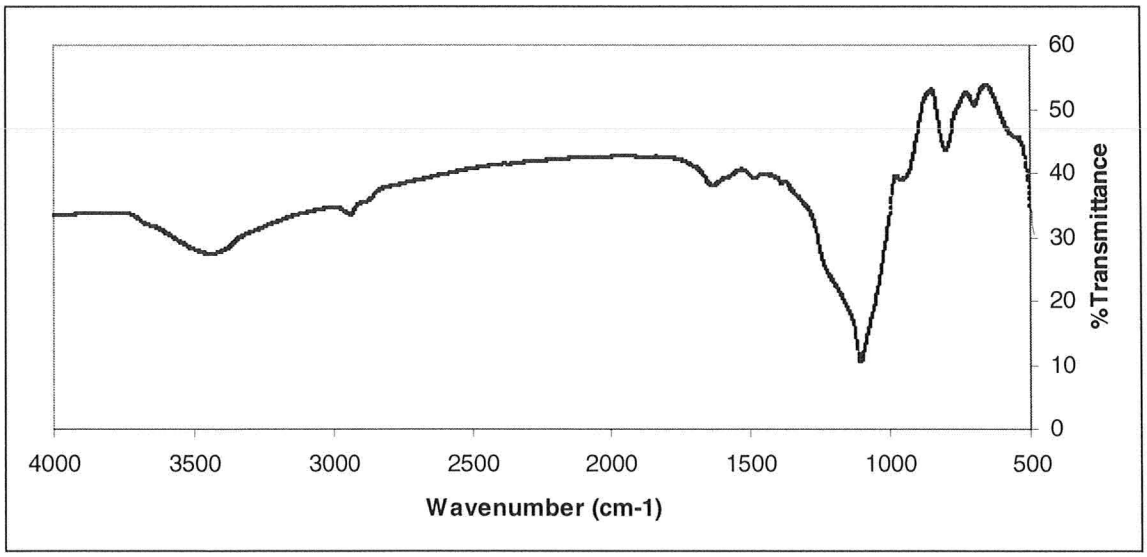

Figure4.6 FTIR spectra of amino silane modified silica nanoparticles

The absorption bands at 1510 cm^{-1} represents the NH_2 vibrations. Intensive band at 1100-1200 cm^{-1} represent the asymmetric stretching of siloxane groups (Si-O-Si). Vibrations at 3400-3500, 1630 and 810 cm^{-1} assigned to the adsorbed water (OH-H, stretching vibration), residual intermolecular water and moisture (H-OH, bending) in the samples [13, 20]. The above picks indicate the achievement of amino functionalization of the nano-silica.

4.4.2.7 Flotation by employing amino silane functionalized silica nanoparticle

Flotation experiemnts of glass beads have been carried out by employing amino silane modified silica nanoparticles as collectors. Results are available in Figure 4.7.

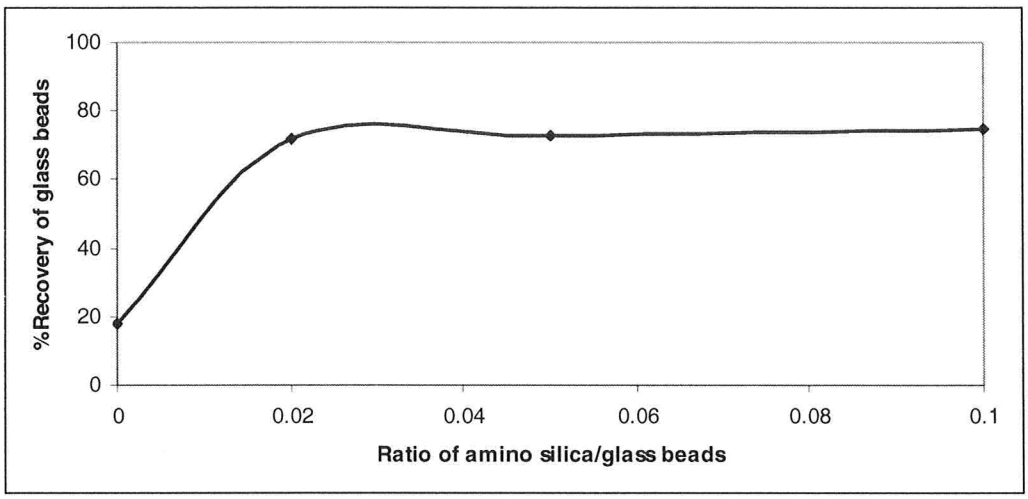

Figure4.7 Flotation of glass beads with amino silane functionalized silica nanoparticle

Figure 4.7 shows that employing amino-silica nanoparticles as flotation collectors does not work satisfactory. It might come from the hydrophilic nature of these nanoparticles which cannot deposit to glass beads appropriately. Therefore, recovery percentage of glass beads is not in an acceptable range. Based on these results, it sounds that the silane group should have a longer alkyl group to give more hydrophobic characteristics to silica nanoparticle. The mercapto silane modified silica nanoparticle can be employed as a flotation collector for pentlandite since it has the same functional groups as xanthate collectors. Therefore, they can have chemical bonds with the minerals and anchor to them.

4.5 CONCLUSION

Stearic acid treated PCC nanoparticles have been synthesized and characterized. Water contact angle measurements showed the hydrophobic characteristic of these nanoparticles. Also, FTIR experiments confirmed chemical structure of these particles.

Moreover, flotation experiments showed very good results when stearic acid treated PCC nanoparticles have been employed as flotation collector which could be related their hydrophobic characteristics and nano size.

Furthermore, silica nanoparticles have been synthesized successfully in Stober method and modified with amino silane and mercapto silane in solvent and also aqueous media with post-modification and co-condensation methods.

The DLS results showed that they are all in the nano particle size range. Also, FTIR experiments confirmed the existence of amino functionalized silica nanoparticles. On the other hand, flotation results are not very good which could be related to hydrophilic characteristics of these nanoparticles. The hydrophobic characteristics could be achieved by increasing the length of alkyl group in silane moieties.

4.6 References:

1. Cho, K.; Saheb, D. N.; Choi, J.; Yang, H., Polymer **2002**, 43, 1407-1416.
2. Guo, T.; Wang, L.; Zhang, A.; Cai, T., J. Appl. Polym. Sci. **2005**, 97, 1154-1160.
3. Wang, C.; Sheng, Y.; Zhao, X.; Pan, Y.; Hari-Bala, Wang, Z., Mat. Letters **2006**, 60, 854-857.
4. Xiang, L.; Xiang, Y.; Wang, Z.G.; Jin, Y., Powder Tech. **2002**, 126, 129-133.
5. Tai, C.Y.; Chen, P.C.; AIChE J. **1995**, 41, 68-77.
6. Lam, T.D.; Hoang, T.V.; Quang, D.T.; Kim, J.S., Mat Sci Eng A **2009**, 501, 87-93.
7. Kim, J.W.; Kim, L.U.; Kim, C.K., Biomacromolecules **2007**, 8, 215.
8. Ijima, M.; Tsukada, H.; Kamiya H., J. Colloid Interface Sci. **2007**, 307, 418.
9. Sun, Y.Y.; Zhang, Z.Q.; Wong, C.P., J. Colloid Interface Sci. **2005**, 292, 436.
10. Kamiya, H.; Mitsui, M.; Takano, H.; Miyazawa, S., J. Am. Ceram. Soc. **2000**, 83, 287.
11. Trappe, V.; Sandkuhler, P., Curr. Opin. Colloid Interface Sci **2004**, 8, 494.
12. Hoffmann, F.; Cornelius M.; Morell J.; Froba, M., Angew. Chem. Int. **2006**, 45, 3216-3251.
13. Rahman, I.A.; Jafarzadeh, M.; Sipaut, C.S., Ceramics Inter. **2009**, 35, 1883-1888.
14. Stober, W.; Fink, A.; Bohn, E., J. Colloid Interface Sci. **1968**, 26, 62-69.
15. Zhao, W.; Pacard, E.; Chaix-Bauvais, C.; Pichot, C.; Brook, M.A., Coll. Surf. A: Phys. Eng. Asp. **2009**, 339, 26-34.
16. Pham, K. N.; Fullston, D.; Sagoe-Crentsil, K., Aust. J. Chem. **2007**, 60, 662-666.
17. Goa, Y.; Huang, Y.; Feng, S.; Gu, G.; Qing, F.L., J. Mater. Sci. **2010**, 45, 460-466.
18. Antunes, E.; Garcia, F.A.P.; Ferreira, P.; Rasteiro, M.G., Chem. Eng. Research & Design **2008**, 86, 1155-1160.
19. Sheng, Y.; Zhou, B.; Wang, C.; Zhao. X.; Deng, Y.; Wang, Z., Applied Surface Science **2006**, 253, 1983-1987.
20. Vandenberg, E.T.; Bertilsson, L.; Liedberg, B.; Uvdal, K.; Erlandsson, R.; Elwing, H.; Lundstorm, I.; J. Colloid Interface Sci. **1991**, 147.